Visibility Laboratory
University of California
Scripps Institution of Oceanography
San Diego 52, California

# A COMPUTER TREATMENT OF RADIATIVE TRANSFER ON A CUBIC LATTICE (PLANE SOURCES)

William Hadley Richardson
and
Rudolph W. Preisendorfer

June 1960
Index Number NS 714-100

SIO REFERENCE 60-46

Bureau of Ships
Contract NObs-72092

Project S F001 05 01

Approved:

Seibert Q. Duntley, Director
Visibility Laboratory

Approved for Distribution:

Roger Revelle, Director
Scripps Institution of Oceanography

# A COMPUTER TREATMENT OF RADIATIVE TRANSFER ON A CUBIC LATTICE (PLANE SOURCE)

## TABLE OF CONTENTS

Table of Contents (Cont'd)

# A COMPUTER TREATMENT OF RADIATIVE TRANSFER ON A CUBIC LATTICE (PLANE SOURCES)

By

William Hadley Richardson and Rudolph W. Preisendorfer

Scripps Institution of Oceanography, University of California

La Jolla, California

## INTRODUCTION

The theory of radiative transfer, which describes the flow of radiant energy through the atmosphere, sea, and other optical media, is at present a theory of increasing importance in those branches of geophysics concerned with atmospheric and hydrologic optics. Despite its phenomenological nature and its outwardly simple appearance, it is a theory of potentially great complexities. These complexities must be borne and resolved if the theory is to fulfill its purpose of giving useful answers to the everyday problems associated with the penetration of light and other forms of radiant energy through the gaseous and liquid optical media mantling the earth.

The heart of radiative transfer theory resides in the integro-differential equation

$$\frac{\eta^2}{V}\,\frac{D[N/\eta^2]}{Dt} = -\alpha N + \int_{\Xi} N\sigma\, d\Omega + N_0 \qquad (*)$$

which describes the spatial and directional evolution of the radiance N of radiant flux at each point of an optical medium X. Within its mathematical form is locked answers to thousands of important questions concerning the why and how of the transfer of radiation through the skies and seas.

Now, because of the equation's relatively intractable structure, most of these answers are still tightly locked from the view of even the practiced eyes of mathematicians armed with the most delicate and incisive of analytic tools. Furthermore, because of its rather fragile structure, it shatters into sterile fragments in the hands of impatient physicists who pry at it with the crowbar of simplifying assumptions. Between these two extreme methods of analysis lies a large, relatively unexplored collection of analytic techniques of intermediate delicacy and incisiveness which may be used to coax the rich store of answers from the equation.

The purpose of this report is to study the numerical application of one such technique. This technique is called <u>discrete-space radiative transfer theory</u> and, in essence, adopts the following point of view: Since the equation of transfer's latent store of information is hopelessly destroyed by any attempt to simplify its structure through tampering with its two inherent optical property functions $\alpha$ and $\sigma$, or by making impossible demands of the directional and spatial structure of the function N itself, these

three functions are to be left strictly alone; instead, if there is going to be any tinkering with the mathematical model represented by (*), it should be with the geometric structure of the optical medium X on which (*) is defined. Thus, in particular, the discrete transfer theory replaces the customary continuum of points of X by a discrete set of points which in principle is at most countably infinite, and in practice merely finite.

The net result of this space-modifying procedure (as contrasted with the process-modifying procedures which affect N, $\alpha$ and $\sigma$ ) is a very tractable mathematical model of radiative transfer processes which possesses an inordinately high fidelity with respect to the natural phenomena it is to describe. Perhaps the most salient property of the discrete space model is its amenability to study by means of large scale automatic computers. The present report gives the results of such a study. These results along with all the relevant details leading to their acquisition, are summarized below. They show that the fruitfulness of the discrete-space approach, which already emerged in the theoretical studies, appears once again on the practical, numerical level.

# A COMPUTER TREATMENT OF RADIATIVE TRANSFER ON A CUBIC LATTICE (PLANE SOURCES)

By

William Hadley Richardson and Rudolph W. Preisendorfer

Scripps Institution of Oceanography, University of California
La Jolla, California

## 1.0 THE PROBLEM

The objectives of this study were:

1.1 A solution on discrete space of the radiative transfer problem using a high speed automatic computer and applying the method developed in reference 1 for a plane parallel source.

1.2 A demonstration of the validity of the solution by applying it to measured initial conditions of a natural case (Reference 2 and 3) and comparing the results of the computed solution with the experimental data.

## 2.0 ASSUMPTIONS

2.1 The basic assumption was that the method is practical for computer adaptation and is a suitable mathematical model.

2.2 It was also assumed that the demonstration of close comparison of analytically computed results with measured data would be an indication of the validity of both the method and this particular adaption.

2.3 The time limitations on production of a solution necessitated the restriction to a homogeneous medium and to considering transmittance within the medium, i.e. not considering boundary conditions such as surface and bottom effects. However the possibility of later development of the solution to include boundary conditions and to apply to a stratified medium were a constant consideration throughout this work.

## 3.0 FACTS BEARING ON THE PROBLEM

3.1 The computer used was the Navy Electronics Laboratory Burroughs Electrodata Datatron 220 which is a general purpose, internally programmed, automatic, digital computer of intermediate size. Currently it may be considered a high speed computer. It has a magnetic core internal memory of 5000 words. It has the following peripheral equipment available for this problem:

Optical reader for punched paper tape
Paper tape punch
Card reader (IBM 087)
Card punch (IBM 523)
Highspeed printer (IBM 407)
Magnetic tape storage units (3), 3,600,000 words total capacity, as tape is blocked for this problem.
Supervisory printer

3.2 The following programming aids were available for this problem:

3.2.1 NEL service routine package, including these subroutines used in this problem: card load; card dump; paper tape dump; magnetic tape store, call, list (Reference 4).

3.2.2 Burroughs matrix operations package, of which these were used: add and subtract, multiply, divide, transpose multiply, inversion by Gauss-Jordan elimination. (Reference 6)

3.2.3 NEL Assembler, an automatic programming system allowing program writing in mnemonic alphabetic command form without addresses and permitting revision by substitution, addition or withdrawal of cards corresponding to steps altered. (Reference 5)

3.2.4 A complete study of radiative optical water properties was available for comparison in the measurements made at Navy Electronics Laboratory Calibration Station, Lake Pend Oreille, Idaho, in 1957 (References 2 and 3) and in 1960 (Appendix A).

## 4.0 DISCUSSION

4.1 The method used in this solution is thoroughly covered in the basic reference 1, and background and development are explained in the supporting references to that paper. Summarizing briefly, the method divides the medium into a cubic lattice and considers the twenty-six directions of the elemental cube (Appendix B) with respect to the center of the cube: each corner, the midpoint of each side and the midpoint of each edge. Since this is a plane-parallel medium the cubes are combined into a series of infinitely continuous slabs, one cube thick. For each slab reflectance and transmittance operators are developed in sequence for downwelling radiance and for upwelling radiance. (Note that in this paper the analogy with the water medium is followed and downwelling is proceeding from zero to depth Z, while upwelling is proceeding from depth Z to zero.) The development of these operators is based on the principles of invariance, the local interaction principle and the eclipse convention. The only input necessary for this determination is the volume (angular) scattering function ($\sigma$) and either the volume attenuation function ($\alpha$) or the volume absorption function (a). and a are interdependent in the relation $\alpha = s + a$, where

$$s = \int_{\Xi} \sigma(\Xi', \Xi)\, d\Omega(\xi)$$

The computational procedure (p. 70 ff. ref. 1) is divided into seven stages:

4.1.1 Stage one: Definition of the quotient space, $Y_{n+2}$, which is the assignment of a depth in optical and linear measure to be considered, division of the space into slabs of arbitrary thickness, definition of the direction space and determination of the local scattering functions $(\Sigma)$ and local absorption function (A).

4.1.2 Stage two: Determination of the matrices for the monolayer reflectance and transmittance operators (R) and (T).

4.1.3 Stage three: Computation in sequence with respect to depth of the reflectance matrices affecting downwelling radiance.

4.1.4 Stage four: Computation in sequence of the reflectance matrices affecting upwelling radiance.

4.1.5 Stage five: Computation in sequence of the transmittance mtrices affecting downwelling radiance.

4.1.6 Stage six: Computation in sequence of the transmittance matrices affecting upwelling radiance.

4.1.7 Stage seven: In which the radiance components in a given slab resulting from radiance sources at the top and bottom of the space are computed by employing the matrices developed in stages three through six. These components are then added to obtain the radiance distribution of the slab under consideration.

4.2 Adaptation to computer operation:

4.2.1 The first step in attacking this problem was to organize it in conformity with the limitations of the 220 computer. Initial memory maps were laid out for the program to include initial data, subroutines and probable working areas. These maps showed that each of stages 3 through 6 would require practically all of the main memory with no space for carry-over storage. This required that at least these stages and probably all stages would have to be programmed as independent phases and that the matrices resulting from each step would have to be stored on magnetic tape as auxiliary storage. In all work consideration had to be given to amending this program to handle non-homogeneous, non-isotropic, bounded media. Keeping this in mind, it was apparent that three magnetic tape units with two lanes each would be required. Fortunately NEL had a third unit on order which was received shortly before the program was ready to be debugged. Further study showed that stages 1 and 2 could be combined temporarily. As finally programmed, this solution consisted of six independent phases, currently designated phases 2 through 7 to correspond to the numbering of stages in the computational procedure, reference 1. Phase 2 combines stage 1 and 2. Following are the memory requirements for each phase as the program now stands.

| Phase | Words |
|---|---|
| 2 | 1943 |
| 3 | 4760 |
| 4 | 4760 |
| 5 | 4713 |
| 6 | 4715 |
| 7 | 4918 |

Maximum internal memory was 5000 words, so it is probable that, in amending, phase 7 will have to be split. Phases 3 through 6 will only require the insertion of a magnetic tape call command to enter the local scattering function ( $\Sigma$ ) for each slab. Phase 2 will certainly become two phases in the non-homogeneous treatment.

Auxiliary magnetic tape storage was assigned with a view to proper sequencing with respect to the production of phases 2, 3, 4, consumption and production of phases 5, 6, 7, so that minimum time would be lost in magnetic tape search. Magnetic tape assignments were:

| Tape | Lane | Matrix |
|---|---|---|
| 1 | 0 | $\Sigma$. (for non-homogeneous case) |
| | 1 | Invariant and M distribution |
| 2 | 0 | R(·, n + 2) |
| | 1 | T(n + 2,·) |
| 3 | 0 | R(·, -1) |
| | | T(-1, ·) |

In thinking of the maximum problem, the limiting element was the $\Sigma$ storage which would hold the solution to a maximum of 877 slabs. Magnetic tapes were preblocked in accordance with Reference 4.b.

Program input was placed on punched paper tape for production. This choice was based on considerations of durability, dependability and control capabilities in comparison with magnetic tape, and speed in comparison with punched cards. The 220 paper tape input is 1000 characters per second while card input is 320 characters per second, and of the latter only 220 per second are program information in the input system used by the service routine. The paper tape was punched by the computer after the program, assembled on cards, had been debugged. Data input was on cards which also controlled the sequencing of problems so that any number of solutions might be run continuously and automatically with no operator supervision or intervention necessary. This choice was made since data preparation on cards was simplest on NEL facilities, and, with the only paper tape reader being used for program input, cards were the only other input available.

Portions of the NEL Service Routine (card load; set memory; card or IBM 407 dump; paper tape dump; and magnetic tape store, call, list) were set into the lowest addresses of all phases, both for program use and for any non-programmed work especially desired during a solution.

In phases 3 through 7 the service subroutines were followed by four Burroughs matrix algebra routines:

$A + B = C$ (C may coincide with A or B);

$AB = C$ (C may coincide with B but not A);

$A^T B = C$ (C may coincide with B but not A);

$A^{-1} = B$ (Gauss-Jordan elimination, B coincides with A)

The use of these routines conserved working space over those allowing no coincidence.

Extracting matrices followed the matrix algebra routines for phases 3 through 6 and were used to extract desired submatrices from the master $\Sigma$ matrix by matrix multiplication (Reference 7). These operators consisted of zero and identity submatrices which by pre- and post-multiplying, with necessary transforming, would strip out a desired submatrix. (See Section 4.2.2)

When programs for all phases had been debugged a punched tape was assembled with each phase in order, with proper control commands so that the program for each phase read in on completion of the preceding phase. Responsibilities of computer operators were limited to loading machine with magnetic tapes, program paper tape, data cards, setting program control switches for desired output and any halts required, and starting paper tape read-in. All other control was in the program or the data cards. By making use of the automatic paper tape rewind, any number of solutions could be run without operator action.

A timing formula for a solution with 407 print-out of the invariant matrix and radiance distribution gave

$$t\ (\text{min}) = 1.52 + 5.33s + 3.28r$$

where t was time in minutes, s was number of slabs, r was number of print-out locations. This has been checked in operation with a maximum proportional error of less than 0.004.

Flow charts for all phases appear in Appendix G.

4.2.2 Computation notes. The use of the Burroughs matrix algebra routines (Reference 6) greatly simplified the programming, since practically all of the computation in Reference 1 was already in matrix form. The routines had a standard entry command format: store re-entry point to base program in routine; branch to routine; define matrices involved by dimension and location; define resultant matrix by dimension and location.

The auxiliary scattering matrices, $s(j,\cdot,\cdot)$ were readily developed from the local scattering function, $(j,\xi_i,\xi_k)$ by the use of the extracting matrices, F(+), F(0), F(-). F(0) = (0,I,0), F(+) = (I,0), and F(-) = (0,I), with the I and 0 matrices of the proper dimensions. These F matrices were fixed in phases 3 through 6. Actually there were also an F(++) = (I,0) which gave a 17 vector output as opposed to a 9 vector output, and an F' = (I,0) which was the contracting matrix, C' = (I,0), (p. 24, ref.1), reducing a 17 vector matrix to a 9 vector matrix.

To use these contraction operators in computing the $S(\cdot\ ,\ \cdot)$ auxiliary scattering matrices (p.45, Ref. 1), the $\Sigma$ matrix was pre-multiplied by the transpose of the F matrix corresponding to the first index in parenthesis in the S( ) term and post-multiplied by the F matrix corresponding to the second index. In this paper an $S(\cdot, ++)$ notation is used to indicate post-multiplication by the $F(++)$ operator to give a 17 vector output. For example: To develop the S(j,0,0) auxiliary matrix, the operation $F^T(0)$ F(0) was executed where F(0) = (0,I,0).

To contract an A', 9 output vector matrix, from an A, 17 output vector matrix, A was post-multiplied by F' corresponding to C in Reference 1.

4.2.3 **Phase 2:** The purpose of this phase (combining stages 1 and 2, in Reference 1,) was to do all preparatory work for the computation of the monolayer operators and the general recurrence relations. In the procedure set up in Reference 1 the monolayer operators would have been computed in this phase, but considerations of time and storage space led to doing monolayer operators as they are needed.

Computer operator responsibility in starting the problem was to set up the three magnetic tape control units, prepare the high speed printer (IBM 407), load data cards into the card reader (IBM 087), load program tape on the optical reader, set control switches for

output and any desired halts, give command for "paper tape read, branch" (0.1000.04.0000). Program was automatic from here on until entire series of problems were completed at which time the supervisory printer would inform the operator.

The paper tape program read in three sections: service subroutines, $\Theta$ matrix, phase two of program. Each section was sum checked and then tape branched to start phase 2.

The first operation in phase 2 was to read in data from cards. These cards were punched in format for the service routine (pp. 4, 5, Reference 4a). The input was (Appendix C): slab definition; volume attenuation function; initial radiance distribution, top and bottom (if radiance output desired); scattering function for the 13 basic angles; problem identification; branch command card to return to problem. At the end of the data cards for a series of problems a control card to branch to problem was inserted. Supervisory pointer announced end of series and computer halts.

The program then computed the total scattering function by numerical integration, the volume absorption function, the slab thickness in linear measure. Then, using the $\Theta$ matrix (Appendix H) which was set up according to p. 63, Reference 1, and read in from tape:

$$\Theta_{ik} = \cos^{-1}(\xi_i \cdot \xi_k) \; ; \; \xi_i, \xi_k \in \Xi'$$

The program manufactured the $\Sigma$ matrix first using the formula:

$$\Sigma(j, \xi_i, \xi_k) = \Delta_j D_i \Omega_i \sigma(z, \xi_i, \xi_k)$$

where $\sigma(z, \xi_i, \xi_k)$ corresponded to the scattering function for $\theta_{ik}$; then adding the diagonal matrix
The Burroughs $e^x$ subroutine was used in this last.

The next computation was the Landau (Hardy) order of magnitude function $o(\alpha(z, \xi_i)\Delta_j)$ , equation (93) Reference 1. This was a measure of the closeness of satisfaction of the local conservation property.

The supervisory printer than announced the input data and the values computed in this phase except for $\Sigma$ . This served as a record that could be included with the print-out and also allowed the operator to check immediately any discrepancies before the problem went much further. See Appendix C, Chart 1.

The program then read in the phase 3 program.

4.2.4 Phase 3: This phase computed the R(•, n + 2) matrix which was the general recurrence relation affecting reflectance of downwelling radiance. The basic equation (p. 98, Reference 1) is:

$$R(n + 2 - p, n + 2) = R(n + 2 - p, n + 3 - p) + T(n + 1 - p, n + 2 - p) \times$$
$$\times [I - R'(n + 3 - p, n + 2) R(n + 2 - p, n + 1 - p)]^{-1} \times$$
$$\times R'(n + 3 - p, n + 2 - p) T(n + 3 - p, n + 2 - p).$$

In somewhat simplified notation this may be written:

$$R(a, n+2) = R(-) + T(-)\underline{I} - R(a+1, n+2)\, R(+)\underline{7}^{-1} x$$

$$x\, R'(a+1, n+2)\, T(+),$$

where a was the slab being computed.

Computation proceeded in sequence from a = n + 1 to a = 0. R(a + 1, n + 2) was held over in storage from the preceding step except for a = n + 1 when the storage space was cleared and represented a zero matrix, since the reflectance of a layer of zero thickness is zero.

The order of calculation of the monolayer terms of the equation and their formulas are:

$$R(+) = S(+,-), + S(+,0)\underline{I} - S(0,0)\underline{7}^{-1} S(0,-)$$

$$T(+) = S(+,++) + S(+,0)\underline{I} - S(0,0)\underline{7}^{-1} S(0,++)$$

$$T(-) + S(-,-) + S(-,0)\underline{I} - S(0,0)\underline{7}^{-1} S(0,-)$$

$$R(-) = S(-,++) + S(-,0)\underline{I} - S(0,0)\underline{7}^{-1} S(0,++)$$

These monolayer R and T operators were calculated and combined as needed. Note that the j in Reference 1 S notation is dropped here and in like expressions in the rest of this paper since the medium was homogeneous. The j may be inferred however and when the program is amended to compute a non-homogeneous medium the only change in steps 3 through 6 will be a command to call a previously computed $\Sigma$ matrix from magnetic tape. The liberty is taken

of introducing an S(·,++) notation to correspond with the F++ extraction operator indicating a 17 output vector matrix while the single + indicates a 9 ouput vector matrix.

As the general recurrence relation for the slab was completed and the result stored on magnetic tape, the program repeated for the next slab until the computation was completed. The supervisory printer announced completion and the next phase was read in from the program paper tape.

4.2.5 Phase 4: This phase was similar to phase 3 and computed R(p-1,-1), the general recurrence relation affecting reflectance of upwelling radiance. The basic equation (p.76, Ref. 1) is:

$$R(p-1,-1) = R(p-1,p-2) + T'(p,p-1)\, x$$
$$x \left[\bar{I} - R(p-2,-1)R'(p-1,p)\right]^{-1} R(p-2,-1)T(p-2,p-1),$$

or simplified:

$$R(a,-1) = R(+) + T'(+)\left[\bar{I} - R(a-1,-1)R'(-)\right]^{-1} R(a-1,-1)T(-),$$

a again was the slab being computed.

Computation proceeded from a = 0 to a = n + 1. R(a-1,-1) was held over in storage from step to step except at a = 0 when a zero matrix appeared in the storage space, as in the similar event in phase 3.

The order of calculation of the monolayer terms and their formulas were:

$$R(-) = S(-,+) + S(-,0)[\bar{I} - S(0,0)]^{-1} S(0,+)$$

$$T(-) = S(-,-) + S(-,0)[\bar{I} - S(0,0)]^{-1} S(0,-)$$

$$T'(+) = S(+,+) + S(+,0)[\bar{I} - S(0,0)]^{-1} S(0,+)$$

$$R(+) = S(+,-) + S(+,0)[\bar{I} - S(0,0)]^{-1} S(0,-)$$

As each slab was completed the result was stored on magnetic tape and the next slab was calculated. When the last slab was completed the supervisory printer announced and the next phase was read from magnetic tape.

4.2.6. Phase 5: This phase was somewhat different from the previous two, and calculated T(-1,p-1), the general recurrence relation affecting transmittance of downwelling radiance. The basic equation is:

$$T(-1,p-1) = T(-1,p-2)[\bar{I} - R'(p-1,p)R(p-2,-1)]^{-1} T(p-2,p-1),$$

or more simply:

$$T(-1,a) = T(-1,a-1)[\bar{I} - R'(-)R(a-1,-1)]^{-1} T(-),$$ a was still the slab being computed.

Computation proceeded from a = 0 to a = n + 1. T(-1, a-1) was held over in storage from step to step except for a = 0 when an identity matrix appeared in the storage space since the transmittance of a slab of zero thickness is unity.

The order of calculation of the monolayer terms and their formulas were:

$$R'(-) = S(-,+) + S(-,0)[I - S(0,0)]^{-1} S(0,+)$$

$$T(-) = S(-,-) + S(-,0)[I - S(0,0)]^{-1} S(0,-)$$

As each slab was completed the result was stored on magnetic tape and the process was repeated for the next slab. When the last slab was completed the supervisoryprinter so informed and the next phase was read from the program tape.

4.2.7 Phase 6: This phase was similar to phase 5, and developed T(n+2, n+2-p) the general recurrence relation affecting transmittance of upwelling radiance. The basic equation is:

$T(n+2, n+2-p) = T'(n+2, n+3-p)[I-R(n+2-p, n+1-p) R'(n+3-p, n+2)]^{-1} x$

$x\ T(n+3-p, n+2-p)$, or more simply:

$T(n+2,a) = T'(n+2,a+1)[I-R(+)R'(a+1, n+2)]^{-1} T(+)$, a was the slab being computed.

Computation proceeded from a = n+1 to a = 0. T(n+2, a+1) was held over in storage from step to step except for a = n + 1 when an identity matrix was introduced into the storage space for the same reason as in phase 5.

The order of calculation of the monolayer terms and their formulas were:

$$R(+) = S(+,-) + S(+,0)[I - S(0,0)]^{-1} S(0,-)$$

$$T(+) = S(+,++) + S(+,0)[I - S(0,0)]^{-1} S(0,++)$$

As each slab was completed the result was stored on magnetic tape and the process repeated for the next slab. The supervisory printer announced completion of the last slab and the optical reader entered the program for phase 7 from the program tape.

4.2.8 Phase 7: In this phase a departure was made from the procedure of Reference 1. The basis was the same but the application used here appeared more suited to computer calculation. The invariant imbedding matrix described in Reference 8 seemed an ideal tool for this phase. This matrix is:

$$M(x,y,z) = \begin{pmatrix} T(z,y,x) & R(z,y,x) \\ R(x,y,z) & T(x,y,z) \end{pmatrix}$$

For our purposes this may be written:

$$M(a) = \begin{pmatrix} T^{+}(a+1) & R^{+}(a) \\ R^{-}(a+1) & T^{-}(a) \end{pmatrix}$$

Here a stood for the slab at the bottom of which the $M$ was computed. In Reference 1, the radiance distribution computed was assumed to be at the center of the slab. In practice this would have resulted in the upward directed radiance at the top boundary of the slab and the downward directed radiance at the bottom boundary. In this problem interest lay in the radiance distribution at an absolute level in the medium, hence the upwelling radiance should be determined at the top of the a + 1 slab and the downwelling at the bottom of the

a slab. The above formula then gives the total distribution at the bottom of the "a" layer, or at a point "a" layers into the medium.

Reference 8 also gives the following equation:

$$[\bar{N} + (y), N-(y)] = [\bar{N} + (z), N-(x)]\mathfrak{M}(x,y,z)$$

This may be written in consistent notation:

$$N(a) = [\bar{N}'+(n+2), N-(-1)]\mathfrak{M}(a)$$

The method used here allowed the four matrices of stage 7, Reference 1, to be represented as a single matrix operator; the two input radiance vectors and the two output vectors to be represented by a single input vector and a single output vector. Finally the radiance distribution was calculated in one step by the operation of the $\mathfrak{M}$ matrix on the N vector instead of the four steps shown in stage 7.

The $\mathfrak{J}$ and $\mathfrak{R}$ submatrices were readily developed by a modification of the method of stage 7. Stripping out the N terms and making appropriate substitutions, equation 102 produced:

$$\mathfrak{J}-(a) = T(-1,a)[\bar{I}-R'(a+1,n+2)R(a,-1)]^{-1}$$

equation 103 became:

$$\mathfrak{R}-(a+1) = T-(a)R(a+1,n+2)$$

and 104:

$$\mathcal{T}+(a+1) = T(n+2,a+1)+T'(n+2,a+1)[I-R(a,-1)R'(a+1,n+2)]^{-1} x$$

$$x\ R(a,-1)R(a+1,n+2)$$

and lastly 105 became:

$$\mathcal{R}+(a) = T+(a+1)R(a,-1)$$

(Note that in the flow chart the script $\mathcal{T}$ and $\mathcal{R}$ were represented by TEE and ARR, $\mathcal{M}$ by INV standing for invariant. This was to correspond with the assembler write-up of the program. The 407 does not print script letters.)

As each of the submatrices was computed it was treated by extension matrices (Reference 7) so as to place it in the proper position in a matrix of the same dimensions as $\mathcal{M}$. Thus:

$$X\mathcal{T}(a) = GM \cdot \mathcal{T}-(a) \cdot HM =$$

$$\begin{pmatrix} 0 \\ I \end{pmatrix} \cdot \mathcal{T}-(a) \cdot (0,I) =$$

$$\begin{pmatrix} 0 & 0 \\ 0 & \mathcal{T}-(a) \end{pmatrix}$$

The other and were treated in similar manner and:

$$\mathcal{M}(a) = X\mathcal{T}-(a) + X\mathcal{R}-(a+1) + X\mathcal{T}+(a+1) + X\mathcal{R}+(a).$$

The X in these equations indicates an extended matrix. G indicates a premultiplying extension operator and H a postmultiplier.

M for - and P for + identifies light direction. Again this was to cope with the limitations of the 407 and is carried over as a standard notation.

Having produced the $\mathfrak{M}$ matrix the N distribution could be computed if desired:

$$N(a) = \angle N' + (n+2),\ N-(-1)\angle \mathfrak{M}(a).$$

In the computer operation, time was saved in case of $N+' = 0$ or $N- = 0$ by control switches which would skip computing the corresponding T and R submatrices. Boundary slabs were handled as in phases 3 through 6 with regard to $\mathfrak{R} = 0$ and $\mathfrak{J} = 1$ in the appropriate submatrices.

All that remained was output of the results. The output was controlled by switches and the possibilities included only practical combination of storing on magnetic tape, printing or abandoning $\mathfrak{M}$ and/or N. See Appendix C for details.

While the R and T operators had to be computed for every slab, $\mathfrak{M}$ and N could be picked out anywhere. In the program, arrangement was then made in initial data for regularly spaced output starting at any desired slab and defining a decreasing slab interval for succeeding outputs. If only one slab was desired, this slab was defined and an interval chosen greater numerically than the number of the slab. In any case, the program would compute each desired slab location in turn and end this phase when it ran out of slabs.

The program then announced end of the problem and read in phase 2 to do another problem. If there were no more problems, after phase 2 had read in, the supervisory printer would announce completion of the series of problems.

If there was need to compute radiance distribution for more than one radiance input vector using the same medium and hence the same $\mathfrak{M}$, the computer had to be stopped at the command to read in phase 2. Then a new radiance input and identification was entered, using the card load service routine, and phase 7 was restarted. There was no need to record $\mathfrak{M}$ again and console switches were set accordingly. Note that if the new N output were stored on magnetic tape it would overwrite the previous N.

Printed output requires some discussion (Appendix D). IBM 407 high speed printer was used with the standard Burroughs 220 general purpose board. The card dump memory list service routine was used to print and automatic switch to memory list was included in the program. Manual switch for memory list could not be used. This switch was used otherwise in this phase. Cardatron format band was included in the program.

Since the matrix algebra routines stored matrices sequentially by column the $\mathfrak{M}$ matrix had to be rearranged to print out properly. The printed output of the 18 x 26 M matrix was ten numbered columns to a page. For the first 25 columns each set of five

columns was treated as a separate submatrix, transposed and transferred to a printout area, so placed that column numbers were in the proper position. Printing five words per line resulted in the desired page format. Column 26 was transferred as was and printed one word per line. This same procedure applied to the 26 element N vector.

When a page of printing was complete, the program branched to turn to next page. It energized tab select relay 1 on the 407, printed a line of zeros and skipped to the next page.

After printing, the 407 sheets could be cut to 8-1/2 x 11 by clipping off the working numbers on the left and the sum check on the right.

In view of the possible range of magnitudes in this problem it was impractical to use decimal notation. The biased 50 floating point notation is cumbersome and may be difficult for the uninitiated. A power of ten notation was used in this printout. The sign digit of a result number was the sign of the exponent, 0 = +, 1 = -, as usual. The first two regular digits were the exponent of 10. The last three digits were the data number with the decimal point before the first of the last three digits. The digit preceding the last three digits was their sign. Thus:

$$-345 = -0.345 \times 10^{3} = 0.0300.00.1345$$

Of course in this computation a negative result would be a danger signal. This process was carried out prior to transferring into print-out arrangement.

In this printout, the first column of the $\mathcal{M}$ carried the slab number, the N vector was headed by its identification, slab number and problem identification.

4.3 Demonstration of Validity. After several shake-down computations to determine effects of varying initial data it was found that, at about a half a slab per optical length, negative elements appeared in the invariant matrix $\mathcal{M}$. These disappeared between one half and one optical length per slab. Varying the optical properties of the medium changed the results in a reasonable manner.

4.3.1 There was a time limitation introduced at this point in the work restricting further work and only a few runs were made at two optical lengths per slab using actual water data for input. Using the measured radiance distribution for a clear, sunny day at Lake Pend Oreille in 1957 and the corresponding attenuation properties measured at the same or similar time, the results shown in Appendix E were obtained.

The scattering function, $\sigma$ , used was measured at Lake Pend Oreille in 1960 two days earlier than the other properties in 1957.

Since other properties measured were somewhat different in the two years, the absorption function, a, was translated from 1957 to 1960 by the relation:

$$\frac{a_1}{a_2} = \frac{K_1}{K_2} \frac{1 - R_{\infty,1}}{1 + R_{\infty,1}} \frac{1 + R_{\infty,2}}{1 - R_{\infty,2}}$$

where K was the K attenuation function (usually considered as for diffuse light) and $R_\infty$ was the ratio of upwelling to downwelling irradiance in an infinitely deep medium. These terms were measured at both times. This translation resulted in a(1960) = 0.200. With $\alpha$(1960) = 0.589, S = $\alpha$ - a = 0.389. The total scattering reduced from nephelometer readings for 1960 was 0.342. There was an element of question as to the true values of the scattering function in, and in the vicinity of, the beam being scattered since the nephelometer does not differentiate between scattered and unscattered light in this region, and measurements in the region are not recorded, but the function is interpolated across the region by a polynomial interpolation. It appeared a reasonable assumption that any difference between values of total scattering obtained analytically and those reduced from measured data could be accounted for in this region. The values of $\sigma$ (0°) and $\sigma$ (10°) were increased so as to be conformable to the rest of the $\sigma$ values and to give a total scattering, S = 0.389. This scattering function was then proportionately reduced, retaining the character of the function, to an S = 0.297, indicated as correct for 1957. The absorption and volume attenuation were as measured in 1957.

The solid angle, $\Delta\Omega$ was assumed in this problem as approximately a spherical quadrilateral with equal sectors of normal great circles as sides. A rough numerical integration was done over this region to determine the input radiance.

4.3.2 The same invariant matrix, $\mathfrak{M}$, was applied to a unit input in each of the three basic downward directions (24, 25, 26, Appendix B). The results are shown in Appendix F. These results clearly showed the rapid attenuation of the unit input element in the shallow region, along with the correspondingly rapid increase in the other two downward directed elements. This result was also a demonstration of the predicted asymptoticity of the attenuation for various directions and the resulting approach to stability in character of the radiance distribution as shown in Reference 9.

## 5. CONCLUSIONS

5.1 General: From the work that has been produced so far with this program, it appears that it gives a good approximate solution to the radiative transfer problem within a homogeneous medium. The results are consonant with theory and are those desired in Reference 1.

5.2 Scattering problem: The results of all production seem to show that the method of reduction of nephelometer measurements does not give a good enough approximation to the true volume scattering function, $\sigma(\theta)$, in the region $\sigma(0^\circ)$ to $\sigma$ (20°). An increase in scattering in this region would increase the ratio of $N_{26}$ to $N_1$ which is now too low in comparison with measured values.

5.3 Value and applications: The program as it now stands can be used to determine analytically the characteristics of radiative transfer in any medium given the volume scattering function and either the absorption or the volume attenuation function, subject to the limitations of plane sources, homogeneity, and transfer within the medium. The program, revised as suggested below in section 5.4, will only have the limitation to plane sources.

5.4 Work remaining:

5.4.1 While the program can now be used to handle any plane source radiative transfer problem within a homogeneous medium there is a certain amount of polishing up of the program that could be done. Slabs per optical length must now be calculated and entered as initial data. By changing the initial data to include the linear measure of range of depth of the problem, this can be handled automatically. Problem identification and slab number should be included in each sheet of the invariant matrix. Optional control should be included to allow automatic computation of additional radiance inputs for the problem medium. Provision should be made to dump the invariant matrix on cards or paper tape for future computation of radiance distributions in the problem medium. A correction should be made to title the input radiance in the check printout on supervisory printer in phase 2. The whole control switch network might well be reworked to give better and more practical and foolproof control. For instance, switch 1 now has two uses in the program, though this is not a great handicap as one function is in phase two and the other much later in phase 7. These are minor amendments and can be done readily.

5.4.2 Major additional work will make the program much more general. While time consuming, programming these revisions and amendments can be done very simply and without changing the general structure of the program.

The solution should handle the boundaries of the medium allowing for a different medium beyond the boundaries, as in the case of a natural body of water the surface and bottom effects should be included. This merely amounts to setting up two special local scattering functions, .

It will be a simple matter to allow for inhomogeneity. The program as now set up allows for this introduction. This will be cared for in what is now phase 2, to be split later into phases 1 and 2. This provision will call for the use of a polynomial curve fitting routine for the volume attenuation function, $\alpha$ and a three variable contouring, or surface fitting, routine for the scattering function, $\sigma(z,\theta)$ . This latter routine is now under development by Burroughs and a prerelease, test copy is on hand here. This will allow a distinct set of initial data including the $\Sigma$ matrix for each slab. This input will be stored on an available lane of magnetic tape and picked up as needed in phases 3 through 6.

5.4.3 Refinement is called for in the integration over the solid angle, $\Delta\Omega$ of the radiance, $N(\theta,\phi)$, $\sigma(\theta)$ and $D(\theta)$. The use of polynomial curve and surface fitting methods will allow input of raw N and $\sigma$ data and permit much more refined and accurate integration of $N$, $\sigma$, and D over the solid angle within the program. The coarse approximations now used are probably the cause of anomalies in results such as the scalloping that appears in the output radiance distribution in the horizontal plane.

# 6. RECOMMENDATIONS

The following are recommended:

6.1 Further refinement and development to generalize the plane source solution to the radiative transfer problem.

6.2 Application of the solution to catalogue a wide range of possible radiance distributions in natural waters and atmospheres, and radiance conditions to support visibility research.

6.3 Development of a generalized point source computer solution to the radiative transfer problem based on Reference 10.

6.4 Further refinement of measurement and reduction techniques in nephelometry. (i.e., the measurement of the volume scattering functions).

## REFERENCES

1. Preisendorfer, R. W., Radiative Transfer on a Cubic Lattice, S.I.O. Ref. 59-68, Scripps Institution of Oceanography, University of California, La Jolla, California (1959).

2. Tyler, J. E., Radiance Distribution as a Function of Depth in an Underwater Environment, Bulletin of the Scripps Institution of Oceanography of the University of California, La Jolla, California, 7, 363 (1960).

3. Duntley, S. Q., Examples of Water Clarity Data, Report 3-7, U.S. Navy Bureau of Ships Project NS 714-100, Contract NObs-72039 (1959).

4. Porter, S. W. and C. B., Service Routine for Burroughs 220 Computer, TM 341, U.S. Navy Electronics Laboratory, San Diego 52, California,(1959).

_____ A System for Block Addressing and Testing a Magnetic Tape for Burroughs 220 Computer, TM 345, U.S. Navy Electronics Laboratory, San Diego 52, California (1959).

5. Barton, L. W., Preliminary Information on 220 Version of 205 Assembler, Unpublished internal memorandum, U.S. Navy Electronics Laboratory, San Diego 52, California (1959).

6. Christopher, J. and Fox, H., Matrix Algebra, Floating Point, Single-precision, Subroutines for the Burroughs 220 Computer,

TB 50, Burroughs Corporation, Electrodata Division, 450 Sierra Madre Villa, Pasadena, California (1959).

7. Richardson, W. H., Extraction and Extension of Matrices in Computer Calculations, SIO Ref. 60-43, Scripps Institution of Oceanography, University of California, La Jolla, California (1960).

8. Preisendorfer, R. W., Invariant Imbedding Relation for the Principles of Invariance, Proc. Natl. Academy of Sciences, 44, 320-323 (1958).

9. _____, A Proof of the Asymptotic Radiance Hypothesis, SIO Ref. 58-57, Scripps Institution of Oceanography, University of California, La Jolla, California (1958).

# APPENDICES

OPTICAL PROPERTIES, NELPOCS, LAKE PEND OREILLE

| | 28 April 1957 | 26 April 1960 |
|---|---|---|
| $\alpha m^{-1}$ | 0.413 | 0.589 |
| $Km^{-1}$ | 0.171 | 0.313 |
| $am^{-1}$ | 0.116 | 0.0607* |
| $R\infty$ | 0.0221 | 0.0509 |
| $Sm^{-1}$ | - | 0.342 |

* This is a questionable value

# THE LOCAL DIRECTION SPACE $\Xi'$

The numbers in the circles correspond to the indices of the elements of $\Xi'$. The circles correspond to the elements of the cell associated with the origin (o,o,o) of $E_3$.

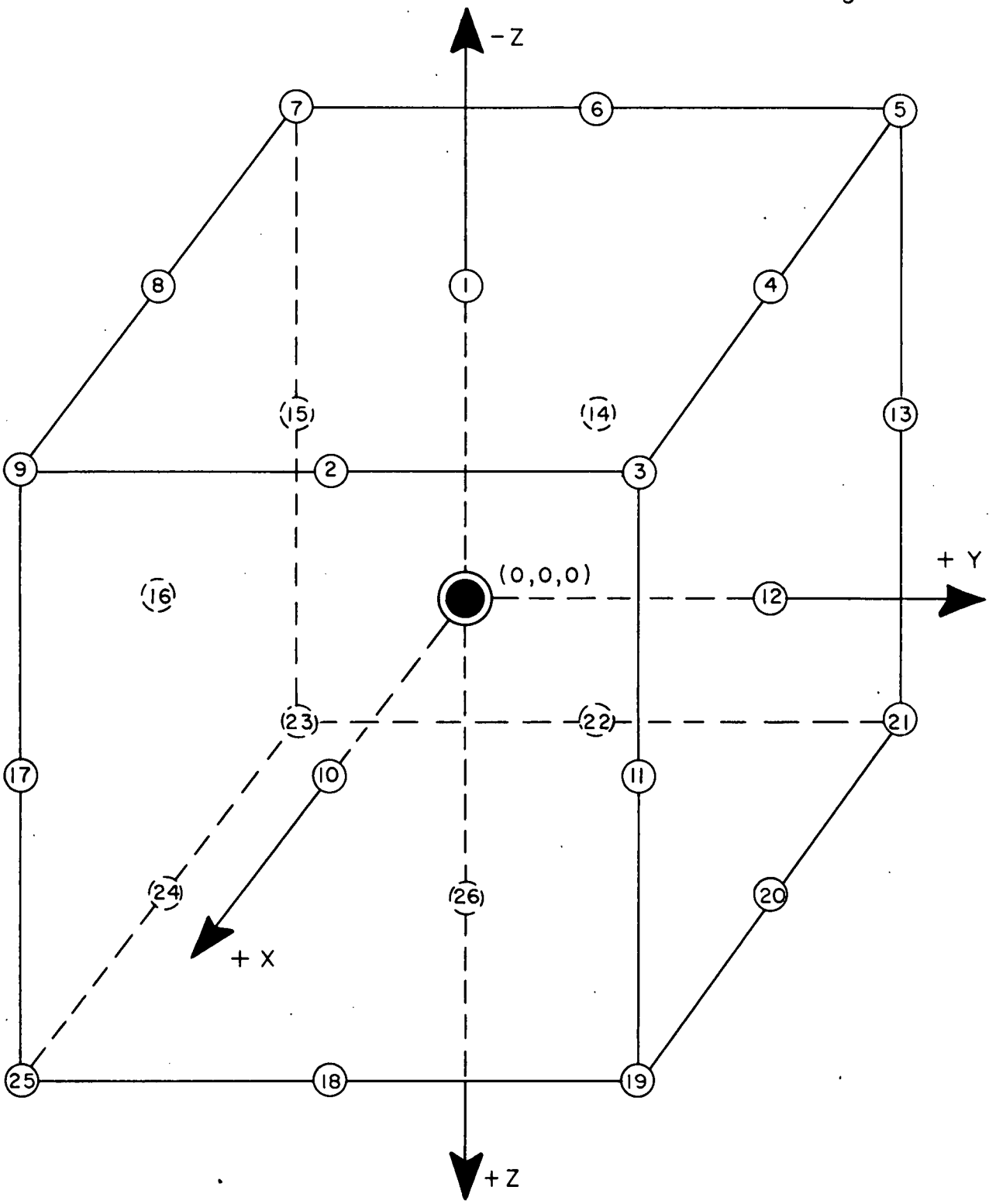


APPENDIX B

# PROGRAM INSTRUCTIONS

Program: Solution to radiative transfer plane source problem

Time required: t(min.) = 1.52 + 5.33 S + 3.28 r

S = number of slabs

r = number of output locations

| | | | | |
|---|---|---|---|---|
| Length of program: | Phase 2 | 628 | Words in locations | 0000-0627 |
| | | 244 | | 2000-2243 |
| | | 1352 | | 2566-3917 |
| | | 49 | | 4900-4948 |
| | | 2273 | | |
| | Phase 3 | 4492 | | 0000-4491 |
| | | 222 | | 4500-4721 |
| | | 49 | | 4900-4948 |
| | | 4763 | | |
| | Phase 4 | 4492 | | 0000-4491 |
| | | 221 | | 4500-4720 |
| | | 49 | | 4900-4948 |
| | | 4762 | | |
| | Phase 5 | 4492 | | 0000-4491 |
| | | 175 | | 4500-4674 |
| | | 49 | | 4900-4948 |
| | | 4716 | | |

APPENDIX C

| | | |
|---|---|---|
| Phase 6 | 4492 | 0000-4491 |
| | 177 | 4500-4676 |
| | 49 | 4900-4948 |
| | 4718 | |
| Phase 7 | 4845 | 0000-4844 |
| | 49 | 4900-4948 |
| | 26 | 4951-4976 |
| | 4920 | |
| TOTAL | 26,152 | |

Peripheral equipment: Optical reader
Supervisory printer set to CR, zero suppress
Magnetic tape control units (3) set to write
Card reader (IBM 087) with general purpose board
High speed printer (IBM 407) with general purpose board

Data input:

| Space | Item |
|---|---|
| 4900 | Number of slabs to be computed less 1 |
| 4901 | Number of slabs per optical length |
| 4902 | Number highest numbered output slab (lowest numbered slab is zero), floating point |
| 4903 | Output slab interval |
| 4904 | $\alpha$, volume attenuation function, floating point |
| 4905 | a, volume absorption function, floating point |
| 4906 | Radiance distribution, 18 numbers starting at $N_1$, floating point |
| 4932 | Scattering function, 13 numbers starting at (0), floating point |
| 4945 | Problem identification (2 words) |

Following the data of each problem, control card:

0.0000.30.2002

Following the complete series, control card:

0.0000.30.2075

APPENDIX C

Output data: On SPO

Identification (2 words)
Number of slabs less 1
Number of slabs per optical length (floating point)
Number of highest numbered output slab
Output slab interval
$\alpha$
S
a
N input (18 numbers)
$\sigma$ (13 numbers)
Landau function, o
$\Delta_j$
} (floating point)
Sigma Complete

On 407

M in 26, numbered, 18 element columns, ten columns to a page. First column headed by the slab number.

N in a 26 element column preceded by
1 - 26
Slab number
Problem identification (2 words)
Blank
26 numbers, $N_1$, ..., $N_{26}$

APPENDIX C

Controls: See Chart 1 for control switches

To start: CLEAR

(rC) = 0.1000.04.0000

EXECUTE

START

To calculate radiance distribution from $N$ in main memory:

During phase 7 set (rS) = 4648

S. to P. : Toggle

N Cards loaded to read in starting at location 4906, followed by control card 0.0000.30.4422

CLEAR (after computer halts)

(rP) = 0020, START

Error halts: a. As listed in Reference 4,a

b. If (rP) indicates halt in matrix algebra routine:

(rD) $\Rightarrow$ (rE) = first address of routine

EXAMINE

(rD) = step following that in which error occurred (last four digits).

APPENDIX C

CONTROL SWITCH CHART

| | 1 | 2 | 3 | 4 | 5 | 6 | 7 | 8 | 9 | 0 |
|---|---|---|---|---|---|---|---|---|---|---|
| Store M | | | | | | | | | | |
| Print M | | | | x | | | | | | |
| Store and print M | | | | | x | | | | | |
| Store M, N | | | | | | x | | | | |
| Print M, N | | | | x | | x | | | | |
| Store print M N | | | | | x | x | | | | |
| Store N | | | x | | | | | | | |
| Print N | | | x | x | | | | | | |
| Store Print N | | | x | | x | | | | | |
| Store M print N | | | x | x | | x | | | | |
| Store M store print N | | | x | | x | x | | | | |
| No upwelling H input | | x | | | | | | | | |
| No downwelling N input | x | | | | | | | | | |
| Halt after phase 2 | x | | | | | | | | | |
| 3 | | | | | | | x | | | |
| 4 | | | | | | | | x | | |
| 5 | | | | | | | | | x | |
| 6 | | | | | | | | | | x |

CHART 1

APPENDIX C

```
   2071960
4000000007
         49
5119580000
         49
         10
ALPHA=  5041300000
S=  5014688734
A=  5026611266
 5010590000
 5016270000
 5020878700
 5015850000
 5019671300
 5015380000
 5019671300
 5015850000
 5020878700
 5716276800
 5617788300
 5580460000
 5535790000
 5541520000
 5535790000
 5580460000
 5617788300
 5697182000
SIGMA FUNCTION
 5030300000
 4945600000
 4916500000
 4873600000
 4853500000
 4828700000
 4812200000
 4784300000
 4780200000
 4779800000
 4782300000
 4784700000
 4791200000
O()=  4912293300
DELTA J =  5112366228
SIGMA COMPLETE
```

(FOR ILLUSTRATION ONLY)

```
0 1000 00 0026   0 0000 00 0-0
0 0000 00 0039   0 0000 00 000
0 0002 07 1960   0 0000 00 000
0 4000 01 0007   0 0000 00 000
0 0000 0  0 0
0 0100 00 0842   0 0000 00 000
0 0200 00 0152   0 0000 00 000
0 0200 00 0161   0 0000 00 000
0 0200 00 0123   0 0000 00 000
0 0200 00 0124   0 0000 00 000
0 0200 00 0103   0 0000 00 000
0 0200 00 0101   0 0000 00 000
0 0100 00 0792   0 0000 00 000
0 0100 00 0563   0 0000 00 000
0 0100 00 0627   0 0000 00 000
0 0200 00 0126   0 0000 00 000
0 0100 00 0643   0 0000 00 000
0 0200 00 0113   0 0000 00 000
0 0100 00 0586   0 0000 00 000
0 0200 00 0103   0 0000 00 000
0 0100 00 0544   0 0000 00 000
0 0100 00 0962   0 0000 00 000
0 0300 00 0114   0 0000 00 000
0 0300 00 0127   0 0000 00 000
0 0300 00 0112   0 0000 00 000
0 0300 00 0114   0 0000 00 000
0 0300 00 0100   0 0000 00 0 0
0 0300 00 0103   0 0000 00 000
0 0200 00 0937   0 0000 00 000
0 0200 00 0951   0 0000 00 000
0 0200 00 0651   0 0000 00 000
0 0000 0  0 0
```

APPENDIX D

| | | | |
|---|---|---|---|
| 0 1111 11 1111 | 0 2222 22 2222 | 0 3333 33 3333 | 0 4444 44 4444 | 0 5555 55 5555 |
| 0 0000 00 0039 | 0 0000 00 000 | | | |
| 1 0200 00 0931 | 1 0200 00 0567 | 1 0200 00 0497 | 1 0200 00 0551 | 1 0200 00 0458 |
| 1 0200 00 0765 | 1 0100 00 0188 | 1 0100 00 0133 | 1 0200 00 0880 | 1 0200 00 0501 |
| 1 0200 00 0786 | 1 0100 00 0171 | 1 0100 00 0188 | 1 0100 00 0152 | 1 0200 00 0779 |
| 1 0200 00 0762 | 1 0100 00 0101 | 1 0100 00 0143 | 1 0100 00 0183 | 1 0100 00 0122 |
| 1 0200 00 0842 | 1 0200 00 0825 | 1 0100 00 0117 | 1 0100 00 0179 | 1 0100 00 0185 |
| 1 0200 00 0795 | 1 0200 00 0598 | 1 0200 00 0710 | 1 0100 00 0106 | 1 0100 00 0141 |
| 1 0200 00 0891 | 1 0200 00 0804 | 1 0200 00 0739 | 1 0200 00 0899 | 1 0100 00 0116 |
| 1 0200 00 0829 | 1 0100 00 0104 | 1 0200 00 0695 | 1 0200 00 0637 | 1 0200 00 0682 |
| 1 0200 00 0931 | 1 0100 00 0186 | 1 0100 00 0115 | 1 0200 00 0836 | 1 0200 00 0671 |
| 1 0500 00 0290 | 1 0500 00 0522 | 1 0500 00 0554 | 1 0500 00 0424 | 1 0500 00 0428 |
| 1 0500 00 0343 | 1 0500 00 0619 | 1 0500 00 0657 | 1 0500 00 0502 | 1 0500 00 0505 |
| 1 0500 00 0281 | 1 0500 00 0506 | 1 0500 00 0539 | 1 0500 00 0412 | 1 0500 00 0414 |
| 1 0500 00 0375 | 1 0500 00 0675 | 1 0500 00 0720 | 1 0500 00 0551 | 1 0500 00 0554 |
| 1 0500 00 0307 | 1 0500 00 0552 | 1 0500 00 0589 | 1 0500 00 0452 | 1 0500 00 0455 |
| 1 0500 00 0417 | 1 0500 00 0749 | 1 0500 00 0799 | 1 0500 00 0613 | 1 0500 00 0619 |
| 1 0500 00 0331 | 1 0500 00 0595 | 1 0500 00 0633 | 1 0500 00 0485 | 1 0500 00 0491 |
| 1 0500 00 0433 | 1 0500 00 0779 | 1 0500 00 0827 | 1 0500 00 0633 | 1 0500 00 0640 |
| 1 0500 00 0145 | 1 0500 00 0261 | 1 0500 00 0277 | 1 0500 00 0212 | 1 0500 00 0214 |
| 0 0000 0 0 0 | | | | |
| 0 6666 66 6666 | 0 7777 77 7777 | 0 8888 88 8888 | 0 9999 99 9999 | 0 1010 10 1010 |
| 0 0000 0 0 0 | | | | |
| 1 0200 00 0522 | 1 0200 00 0426 | 1 0200 00 0485 | 1 0200 00 0382 | 1 0300 00 0352 |
| 1 0200 00 0475 | 1 0200 00 0512 | 1 0200 00 0842 | 1 0100 00 0115 | 1 0200 00 0103 |
| 1 0200 00 0534 | 1 0200 00 0386 | 1 0200 00 0521 | 1 0200 00 0743 | 1 0300 00 0998 |
| 1 0200 00 0794 | 1 0200 00 0413 | 1 0200 00 0377 | 1 0200 00 0407 | 1 0300 00 0664 |
| 1 0100 00 0150 | 1 0200 00 0756 | 1 0200 00 0508 | 1 0200 00 0378 | 1 0300 00 0584 |
| 1 0100 00 0181 | 1 0100 00 0120 | 1 0200 00 0774 | 1 0200 00 0401 | 1 0300 00 0445 |
| 1 0100 00 0178 | 1 0100 00 0184 | 1 0100 00 0149 | 1 0200 00 0754 | 1 0300 00 0580 |
| 1 0100 00 0104 | 1 0100 00 0138 | 1 0100 00 0178 | 1 0100 00 0118 | 1 0300 00 0689 |
| 1 0200 00 0838 | 1 0100 00 0109 | 1 0100 00 0171 | 1 0100 00 0177 | 1 0200 00 0111 |
| 1 0500 00 0356 | 1 0500 00 0347 | 1 0500 00 0273 | 1 0500 00 0194 | 1 0500 00 0217 |
| 1 0500 00 0420 | 1 0500 00 0409 | 1 0500 00 0322 | 1 0500 00 0229 | 1 0500 00 0257 |
| 1 0500 00 0343 | 1 0500 00 0334 | 1 0500 00 0263 | 1 0500 00 0187 | 1 0500 00 0210 |
| 1 0500 00 0459 | 1 0500 00 0446 | 1 0500 00 0350 | 1 0500 00 0249 | 1 0500 00 0278 |
| 1 0500 00 0377 | 1 0500 00 0366 | 1 0500 00 0287 | 1 0500 00 0204 | 1 0500 00 0226 |
| 1 0500 00 0513 | 1 0500 00 0499 | 1 0500 00 0390 | 1 0500 00 0278 | 1 0500 00 0307 |
| 1 0500 00 0408 | 1 0500 00 0397 | 1 0500 00 0311 | 1 0500 00 0221 | 1 0500 00 0245 |
| 1 0500 00 0532 | 1 0500 00 0519 | 1 0500 00 0407 | 1 0500 00 0289 | 1 0500 00 0322 |
| 1 0500 00 0178 | 1 0500 00 0173 | 1 0500 00 0136 | 1 0600 00 0965 | 1 0500 00 0107 |
| 0 0000 0 0 0 | | | | |
| 0 0000 0 0 0 | | | | |

APPENDIX D

| | | | |
|---|---|---|---|
| 0 1100 11 0011 | 0 1212 12 1212 | 0 1313 13 1313 | 0 1414 14 1414 | 0 1515 15 1515 |
| 0 0000 00 0 0 | | | | |
| 1 0300 00 0631 | 1 0300 00 0358 | 1 0300 00 0593 | 1 0300 00 0341 | 1 0300 00 0561 |
| 1 0200 00 0166 | 1 0300 00 0627 | 1 0300 00 0699 | 1 0300 00 0393 | 1 0300 00 0709 |
| 1 0200 00 0231 | 1 0300 00 0950 | 1 0200 00 0104 | 1 0300 00 0442 | 1 0300 00 0578 |
| 1 0200 00 0176 | 1 0200 00 0103 | 1 0200 00 0154 | 1 0300 00 0578 | 1 0300 00 0605 |
| 1 0200 00 0146 | 1 0200 00 0109 | 1 0200 00 0230 | 1 0300 00 0951 | 1 0200 00 0103 |
| 1 0300 00 0919 | 1 0300 00 0722 | 1 0200 00 0175 | 1 0200 00 0103 | 1 0200 00 0154 |
| 1 0300 00 0974 | 1 0300 00 0661 | 1 0200 00 0147 | 1 0200 00 0109 | 1 0200 00 0230 |
| 1 0300 00 0913 | 1 0300 00 0498 | 1 0300 00 0906 | 1 0300 00 0717 | 1 0200 00 0173 |
| 1 0200 00 0146 | 1 0300 00 0641 | 1 0300 00 0921 | 1 0300 00 0635 | 1 0200 00 0141 |
| 1 0500 00 0434 | 1 0500 00 0221 | 1 0500 00 0389 | 1 0500 00 0201 | 1 0500 00 0354 |
| 1 0500 00 0518 | 1 0500 00 0264 | 1 0500 00 0463 | 1 0500 00 0238 | 1 0500 00 0416 |
| 1 0500 00 0424 | 1 0500 00 0217 | 1 0500 00 0383 | 1 0500 00 0196 | 1 0500 00 0341 |
| 1 0500 00 0563 | 1 0500 00 0290 | 1 0500 00 0515 | 1 0500 00 0263 | 1 0500 00 0457 |
| 1 0500 00 0457 | 1 0500 00 0236 | 1 0500 00 0421 | 1 0500 00 0217 | 1 0500 00 0378 |
| 1 0500 00 0617 | 1 0500 00 0319 | 1 0500 00 0569 | 1 0500 00 0295 | 1 0500 00 0517 |
| 1 0500 00 0489 | 1 0500 00 0252 | 1 0500 00 0447 | 1 0500 00 0232 | 1 0500 00 0410 |
| 1 0500 00 0643 | 1 0500 00 0329 | 1 0500 00 0581 | 1 0500 00 0302 | 1 0500 00 0534 |
| 1 0500 00 0216 | 1 0500 00 0111 | 1 0500 00 0196 | 1 0500 00 0101 | 1 0500 00 0178 |
| 0 0000 0 0 0 | | | | |
| 0 1616 16 1616 | 0 1717 17 1717 | 0 1818 18 1818 | 0 1919 19 1919 | 0 2020 20 2020 |
| 0 0000 0 0 0 | | | | |
| 1 0300 00 0323 | 1 0300 00 0524 | 1 0300 00 0320 | 1 0300 00 0455 | 1 0300 00 0300 |
| 1 0300 00 0597 | 1 0200 00 0149 | 1 0300 00 0688 | 1 0300 00 0995 | 1 0300 00 0528 |
| 1 0300 00 0436 | 1 0200 00 0102 | 1 0300 00 0720 | 1 0200 00 0123 | 1 0300 00 0628 |
| 1 0300 00 0343 | 1 0300 00 0616 | 1 0300 00 0599 | 1 0200 00 0104 | 1 0300 00 0629 |
| 1 0300 00 0446 | 1 0300 00 0606 | 1 0300 00 0637 | 1 0200 00 0103 | 1 0300 00 0738 |
| 1 0300 00 0579 | 1 0300 00 0618 | 1 0300 00 0545 | 1 0300 00 0775 | 1 0300 00 0613 |
| 1 0300 00 0960 | 1 0200 00 0106 | 1 0300 00 0664 | 1 0300 00 0861 | 1 0300 00 0663 |
| 1 0200 00 0103 | 1 0200 00 0154 | 1 0300 00 0650 | 1 0300 00 0783 | 1 0300 00 0552 |
| 1 0200 00 0106 | 1 0200 00 0227 | 1 0300 00 0847 | 1 0200 00 0106 | 1 0300 00 0654 |
| 1 0500 00 0188 | 1 0500 00 0333 | 1 0400 00 0395 | 1 0400 00 0439 | 1 0400 00 0385 |
| 1 0500 00 0221 | 1 0500 00 0392 | 1 0400 00 0470 | 1 0400 00 0525 | 1 0400 00 0461 |
| 1 0500 00 0180 | 1 0500 00 0317 | 1 0400 00 0381 | 1 0400 00 0430 | 1 0400 00 0380 |
| 1 0500 00 0240 | 1 0500 00 0421 | 1 0400 00 0504 | 1 0400 00 0570 | 1 0400 00 0508 |
| 1 0500 00 0197 | 1 0500 00 0345 | 1 0400 00 0409 | 1 0400 00 0462 | 1 0400 00 0413 |
| 1 0500 00 0270 | 1 0500 00 0471 | 1 0400 00 0555 | 1 0400 00 0622 | 1 0400 00 0555 |
| 1 0500 00 0215 | 1 0500 00 0377 | 1 0400 00 0444 | 1 0400 00 0493 | 1 0400 00 0437 |
| 1 0500 00 0282 | 1 0500 00 0496 | 1 0400 00 0586 | 1 0400 00 0649 | 1 0400 00 0570 |
| 1 0600 00 0935 | 1 0500 00 0164 | 1 0400 00 0195 | 1 0400 00 0218 | 1 0400 00 0193 |
| 0 0000 0 0 0 | | | | |
| 0 0000 0 0 0 | | | | |

APPENDIX D

| 0 2121 21 2121 | 0 2200 22 0022 | 0 2323 23 2323 | 0 2424 24 2424 | 0 2525 25 2525 |
|---|---|---|---|---|
| 0 0000 00 0 0 | | | | |
| 1 0300 00 0437 | 1 0300 00 0287 | 1 0300 00 0411 | 1 0300 00 0284 | 1 0300 00 0377 |
| 1 0300 00 0644 | 1 0300 00 0459 | 1 0300 00 0640 | 1 0300 00 0532 | 1 0300 00 0867 |
| 1 0300 00 0788 | 1 0300 00 0482 | 1 0300 00 0595 | 1 0300 00 0503 | 1 0300 00 0738 |
| 1 0300 00 0929 | 1 0300 00 0489 | 1 0300 00 0574 | 1 0300 00 0448 | 1 0300 00 0558 |
| 1 0200 00 0125 | 1 0300 00 0644 | 1 0300 00 0795 | 1 0300 00 0542 | 1 0300 00 0606 |
| 1 0200 00 0106 | 1 0300 00 0639 | 1 0300 00 0932 | 1 0300 00 0536 | 1 0300 00 0579 |
| 1 0200 00 0107 | 1 0300 00 0756 | 1 0200 00 0126 | 1 0300 00 0696 | 1 0300 00 0813 |
| 1 0300 00 0794 | 1 0300 00 0618 | 1 0200 00 0105 | 1 0300 00 0665 | 1 0300 00 0925 |
| 1 0300 00 0860 | 1 0300 00 0655 | 1 0200 00 0103 | 1 0300 00 0766 | 1 0200 00 0122 |
| 1 0400 00 0389 | 1 0400 00 0345 | 1 0400 00 0354 | 1 0400 00 0324 | 1 0400 00 0330 |
| 1 0400 00 0464 | 1 0400 00 0407 | 1 0400 00 0414 | 1 0400 00 0378 | 1 0400 00 0387 |
| 1 0400 00 0385 | 1 0400 00 0336 | 1 0400 00 0339 | 1 0400 00 0307 | 1 0400 00 0313 |
| 1 0400 00 0519 | 1 0400 00 0454 | 1 0400 00 0456 | 1 0400 00 0410 | 1 0400 00 0413 |
| 1 0400 00 0424 | 1 0400 00 0375 | 1 0400 00 0379 | 1 0400 00 0339 | 1 0400 00 0339 |
| 1 0400 00 0572 | 1 0400 00 0509 | 1 0400 00 0519 | 1 0400 00 0465 | 1 0400 00 0464 |
| 1 0400 00 0449 | 1 0400 00 0401 | 1 0400 00 0411 | 1 0400 00 0372 | 1 0400 00 0373 |
| 1 0400 00 0582 | 1 0400 00 0519 | 1 0400 00 0534 | 1 0400 00 0486 | 1 0400 00 0492 |
| 1 0400 00 0197 | 1 0400 00 0175 | 1 0400 00 0178 | 1 0400 00 0161 | 1 0400 00 0162 |
| 0 0000 0 0 0 | | | | |
| 0 2626 26 2626 | 0 0000 00 000 | | | |
| 0 0000 0 0 0 | | | | |
| 1 0300 00 0174 | 0 0000 00 000 | | | |
| 1 0300 00 0325 | 0 0000 00 000 | | | |
| 1 0300 00 0335 | 0 0000 00 000 | | | |
| 1 0300 00 0304 | 0 0000 00 000 | | | |
| 1 0300 00 0354 | 0 0000 00 000 | | | |
| 1 0300 00 0324 | 0 0000 00 000 | | | |
| 1 0300 00 0392 | 0 0000 00 000 | | | |
| 1 0300 00 0362 | 0 0000 00 000 | | | |
| 1 0300 00 0432 | 0 0000 00 000 | | | |
| 1 0400 00 0225 | 0 0000 00 000 | | | |
| 1 0400 00 0266 | 0 0000 00 000 | | | |
| 1 0400 00 0218 | 0 0000 00 000 | | | |
| 1 0400 00 0291 | 0 0000 00 000 | | | |
| 1 0400 00 0238 | 0 0000 00 000 | | | |
| 1 0400 00 0323 | 0 0000 00 000 | | | |
| 1 0400 00 0256 | 0 0000 00 000 | | | |
| 1 0400 00 0335 | 0 0000 00 000 | | | |
| 1 0400 00 0112 | 0 0000 00 000 | | | |
| 0 0000 0 0 0 | | | | |
| 0 0000 0 0 0 | | | | |
| 0 0000 0 0 0 | | | | |
| 0 0000 0 0 0 | | | | |
| 0 0000 0 0 0 | | | | |

APPENDIX D

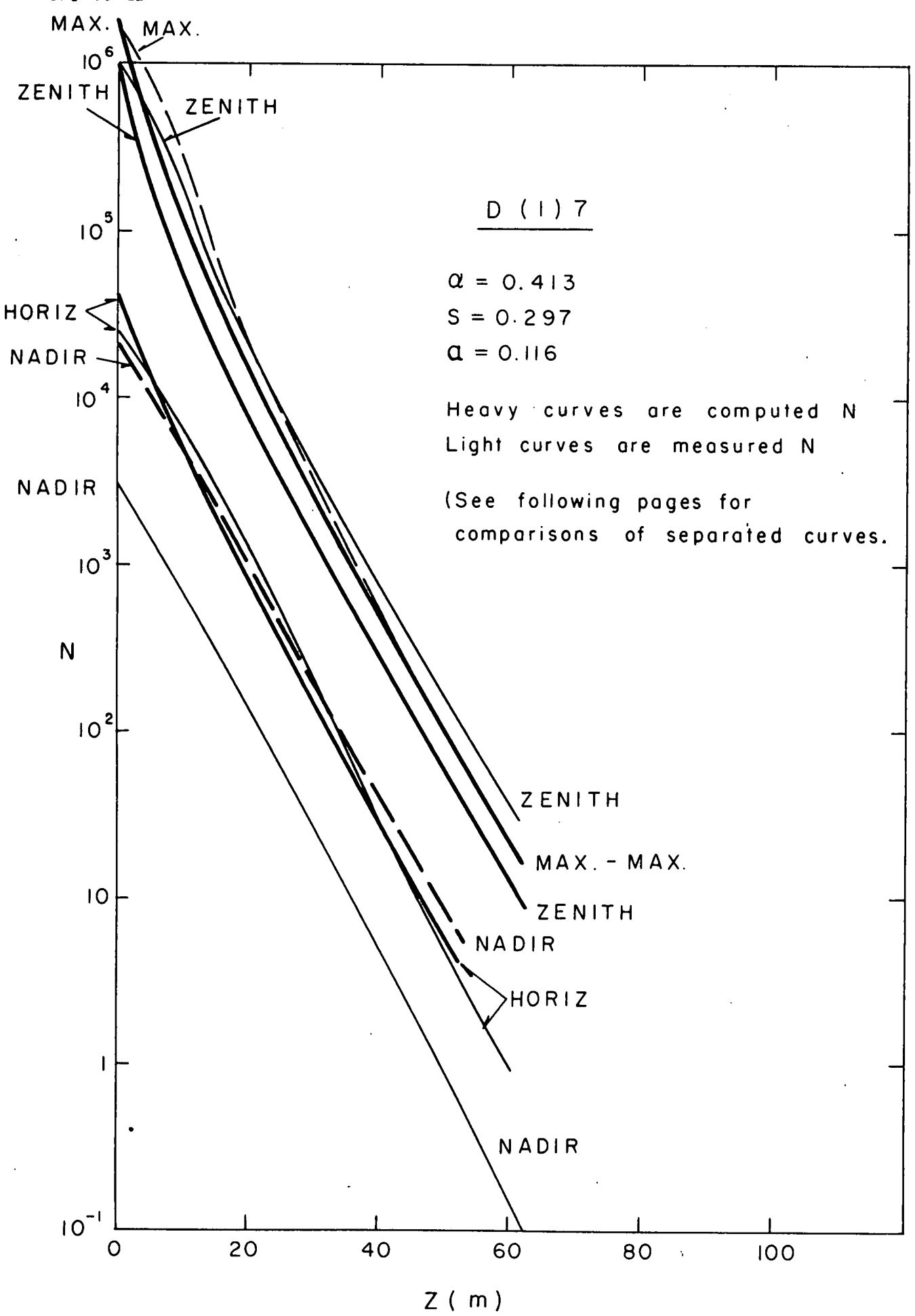
MAX.
MAX.
ZENITH
ZENITH
HORIZ
NADIR
NADIR
D (1) 7
α = 0.413
S = 0.297
a = 0.116
Heavy curves are computed N
Light curves are measured N
(See following pages for comparisons of separated curves.
ZENITH
MAX. - MAX.
ZENITH
NADIR
HORIZ
NADIR
N
Z (m)
$10^6$
$10^5$
$10^4$
$10^3$
$10^2$
10
1
$10^{-1}$
0
20
40
60
80
100

APPENDIX E

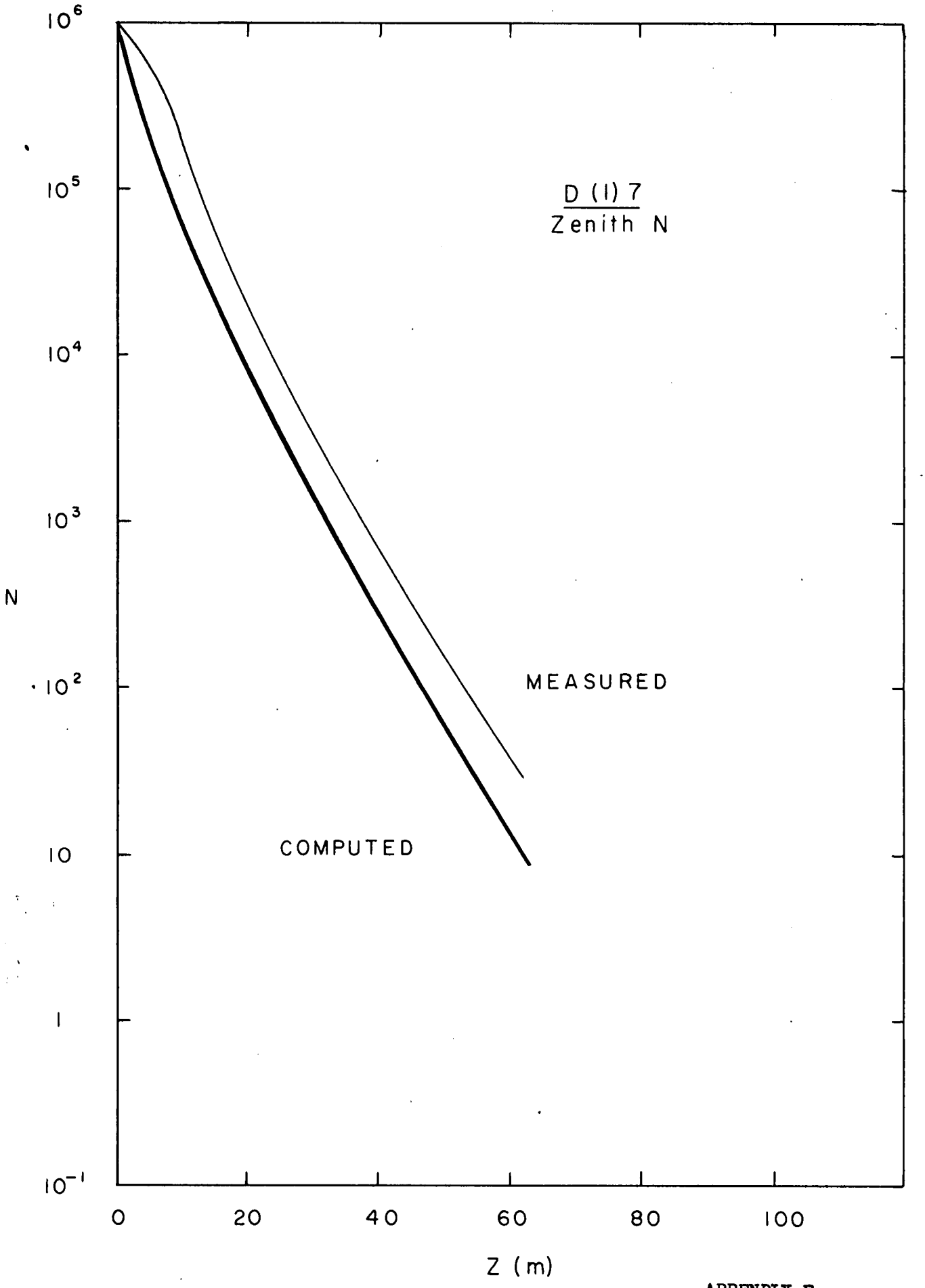
$10^6$
$10^5$
$10^4$
$10^3$
N
$10^2$
10
1
$10^{-1}$
D (1) 7
Zenith N
MEASURED
COMPUTED
0
20
40
60
80
100
Z (m)

APPENDIX E

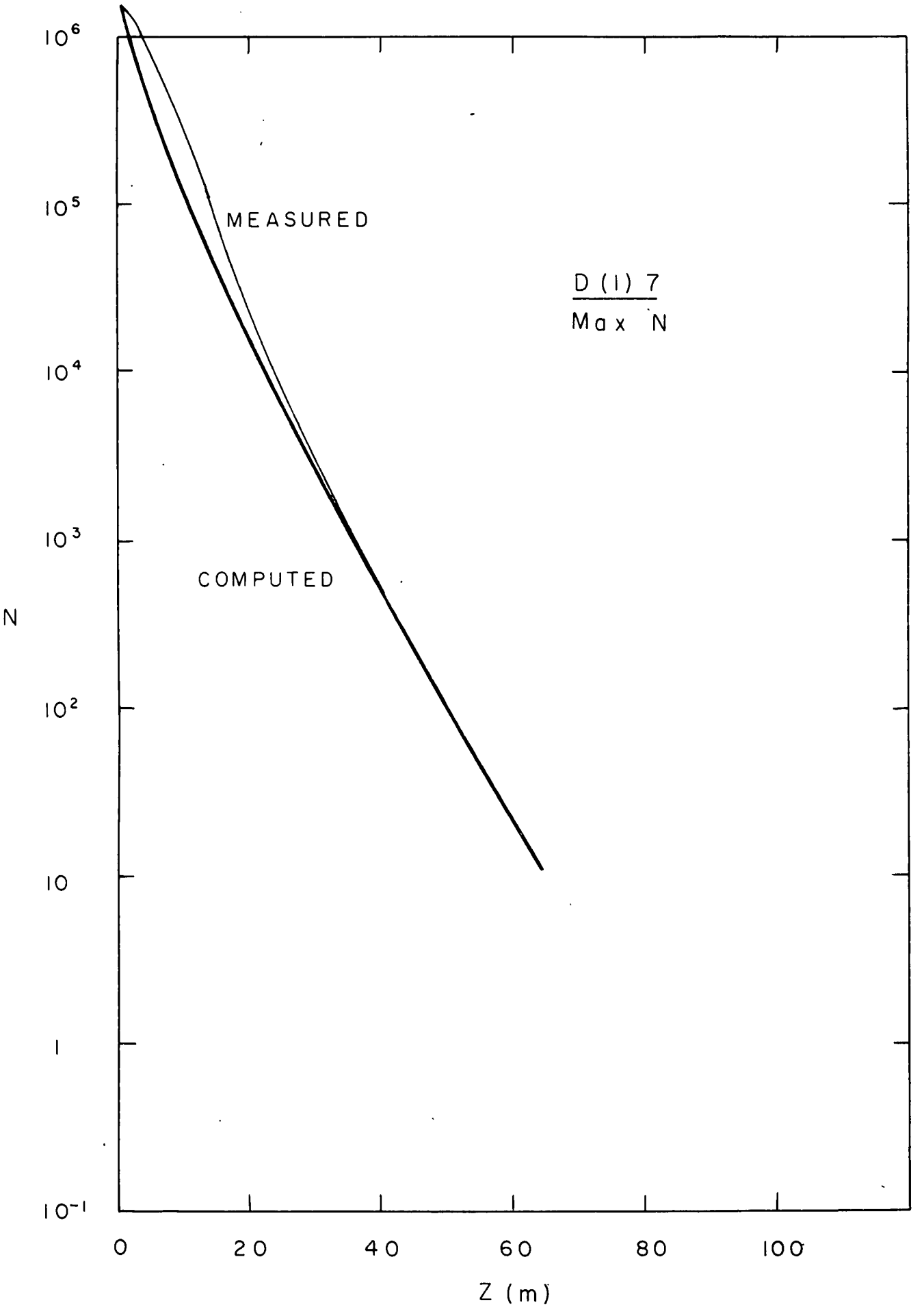
$10^6$
$10^5$
$10^4$
$10^3$
$10^2$
10
1
$10^{-1}$
N
MEASURED
COMPUTED
D (1) 7
Max N
0
20
40
60
80
100
Z (m)

APPENDIX E

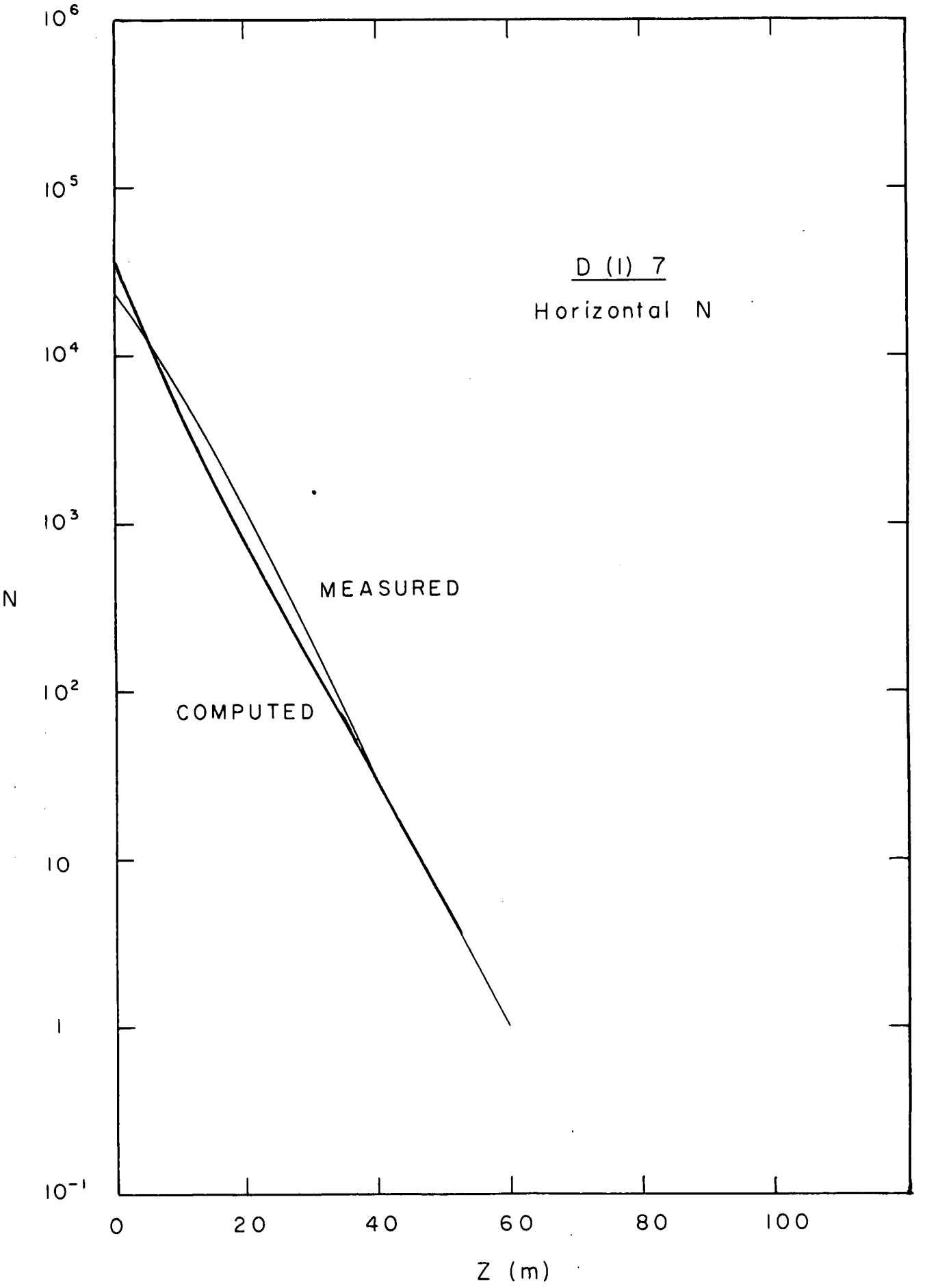
D (I) 7
Horizontal N
MEASURED
COMPUTED
N
Z (m)
$10^6$
$10^5$
$10^4$
$10^3$
$10^2$
10
1
$10^{-1}$
0
20
40
60
80
100

APPENDIX E

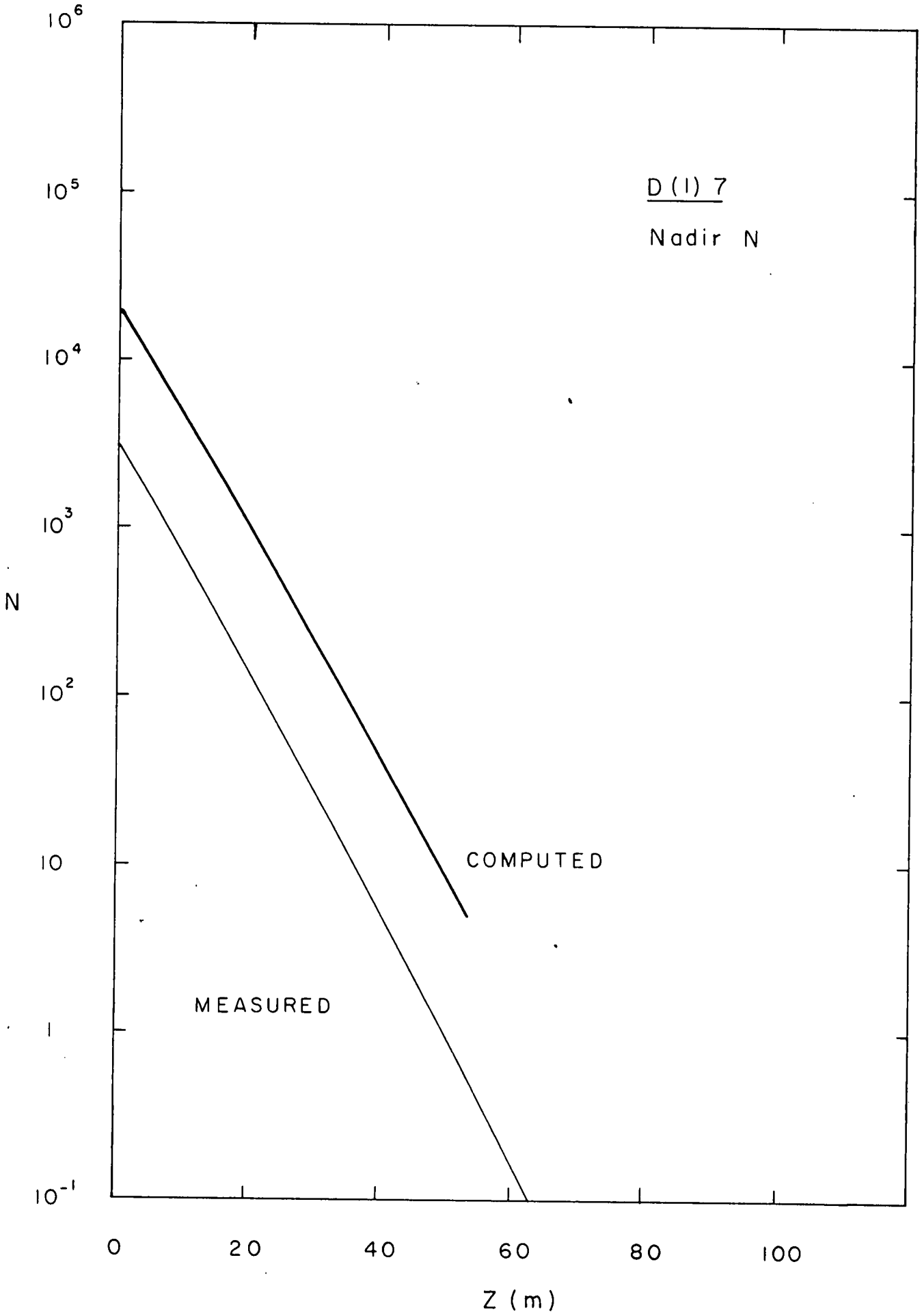
D(1) 7
Nadir N
COMPUTED
MEASURED
N
Z (m)
$10^6$
$10^5$
$10^4$
$10^3$
$10^2$
10
1
$10^{-1}$
0
20
40
60
80
100

APPENDIX E

D (1) 7

| Slab | Z(M) | $N_1$ | $N_{10}$ | $N_{18}$ | $N_{26}$ |
|---|---|---|---|---|---|
| -1 | 0 | 21 400 | 41 300 | 1 630 000 | 972 000 |
| 9 | 12.4 | 3 230 | 2 930 | 60 300 | 29 600 |
| 19 | 24.7 | 447 | 348 | 6 520 | 3 440 |
| 29 | 37.1 | 61.8 | 46.1 | 843 | 472 |
| 39 | 49.5 | 8.42 | 6.27 | 114 | 65.1 |
| 49 | 61.8 | 0.106 | - | 15.6 | 8.95 |

| | |
|---|---|
| o ( ) | - 0.147 |
| /m | 0.413 |
| S /n | 0.297 |
| a/n | 0.116 |
| K/m | 0.188 |
| R/m | 0.0220 |
| slab/L$\alpha$ | 1.958 |
| L$\alpha$ | 2.42m |
| $\Delta$ j | 1.237m |

APPENDIX E

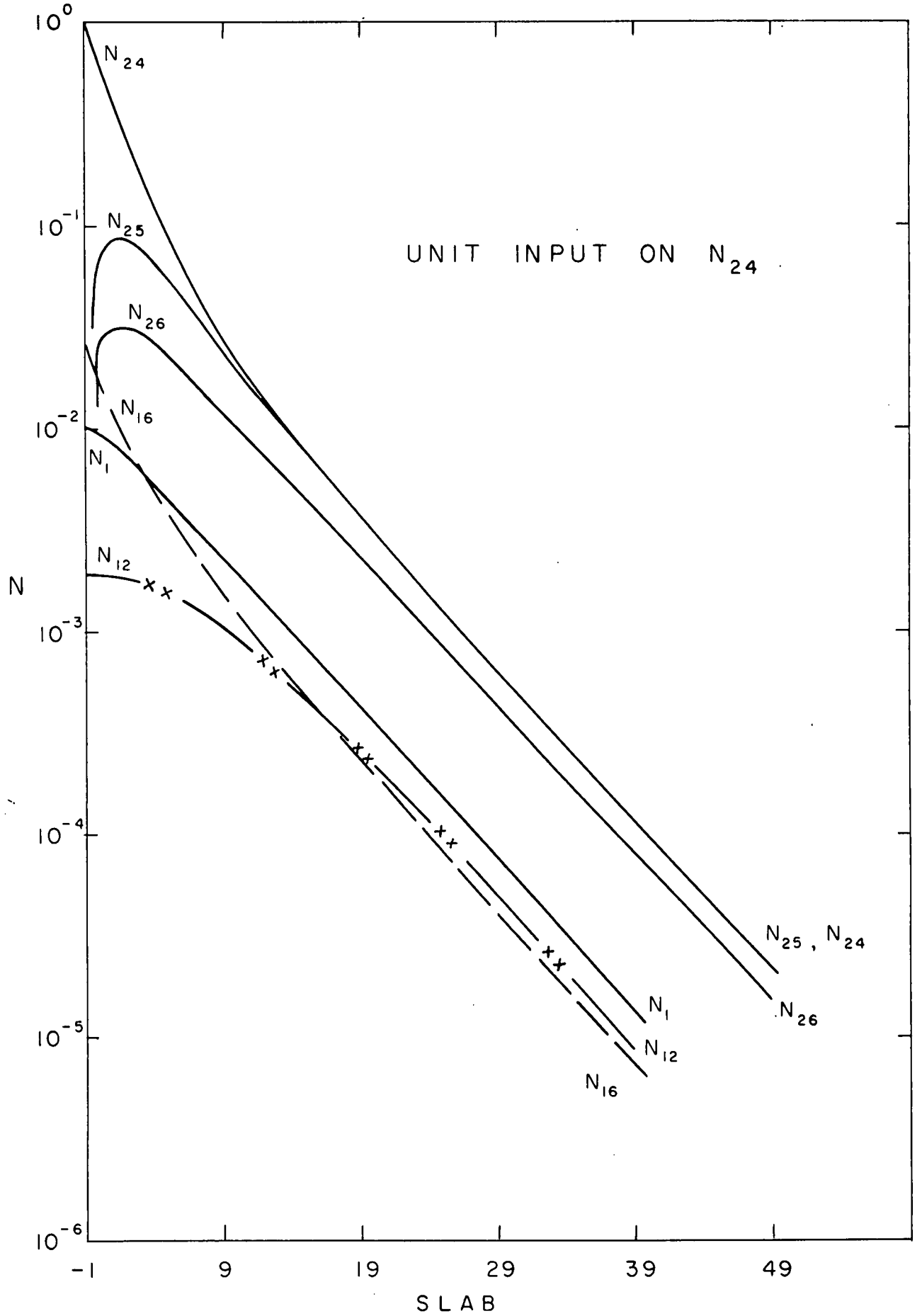
UNIT INPUT ON $N_{24}$
$N_{24}$
$N_{25}$
$N_{26}$
$N_{16}$
$N_1$
$N_{12}$
$N_{25}$ , $N_{24}$
$N_{26}$
$N_1$
$N_{12}$
$N_{16}$
N
$10^0$
$10^{-1}$
$10^{-2}$
$10^{-3}$
$10^{-4}$
$10^{-5}$
$10^{-6}$
-1
9
19
29
39
49
SLAB

$N_{24}$

| Slab | $N_1$ | $N_{12}$ | $N_{16}$ | $N_{24}$ | $N_{25}$ | $N_{26}$ |
|---|---|---|---|---|---|---|
| -1 | 0.010 6 | 0.001 92 | 0.023 2 | 1.000 | 0 | 0 |
| 0 | 0.009 47 | 0.001 90 | 0.016 2 | 0.608 | 0.068 4 | 0.024 1 |
| 1 | 0.008 25 | 0.001 88 | 0.011 6 | 0.383 | 0.088 4 | 0.031 8 |
| 2 | 0.007 10 | 0.001 84 | 0.008 54 | 0.251 | 0.087 3 | 0.032 4 |
| 3 | 0.006 07 | 0.001 77 | 0.006 43 | 0.170 | 0.078 0 | 0.030 0 |
| 4 | 0.005 16 | 0.001 67 | 0.004 94 | 0.119 | 0.066 5 | 0.026 6 |
| 9 | 0.002 25 | 0.001 04 | 0.001 58 | 0.029 4 | 0.024 9 | 0.012 3 |
| 19 | 0.000 421 | 0.000 250 | 0.000 238 | 0.003 85 | 0.003 74 | 0.002 34 |
| 29 | 0.000 078 3 | 0.000 049 2 | 0.000 041 7 | 0.000 654 | 0.000 657 | 0.000 438 |
| 39 | 0.000 014 2 | 0.000 009 24 | 0.000 007 62 | 0.000 119 | 0.000 121 | 0.000 081 5 |
| 49 | - | - | - | 0.000 021 7 | 0.000 022 1 | 0.000 015 0 |

APPENDIX F

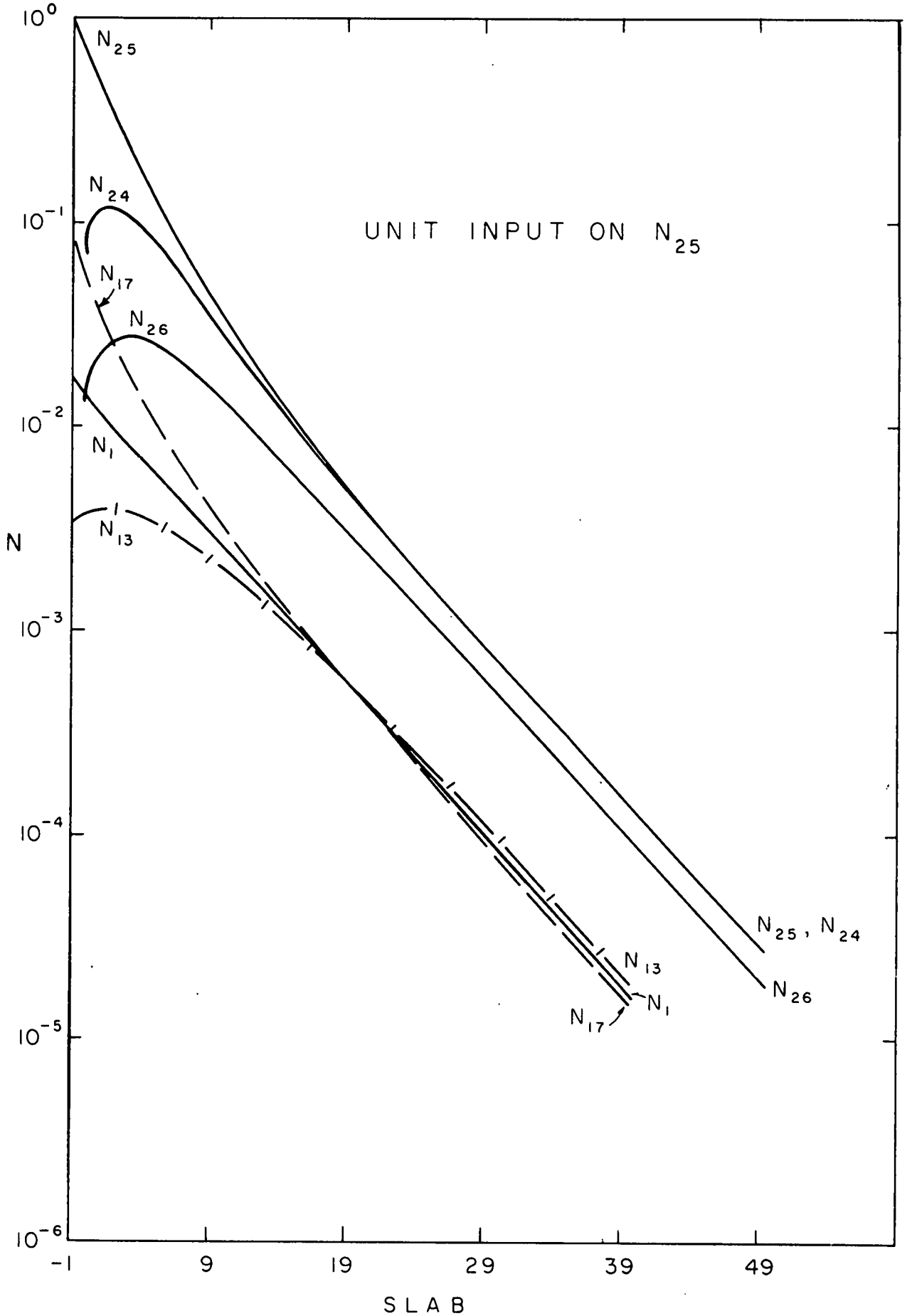
UNIT INPUT ON N25
N25
N24
N17
N26
N1
N13
N
10^0
10^-1
10^-2
10^-3
10^-4
10^-5
10^-6
-1
9
19
29
39
49
SLAB
N25 , N24
N26
N13
N1
N17

$N_{25}$

| Slab | $N_1$ | $N_{15}$ | $N_{17}$ | $N_{24}$ | $N_{25}$ | $N_{26}$ |
|---|---|---|---|---|---|---|
| -1 | 0.017 3 | 0.003 40 | 0.077 8 | 0 | 1 | 0 |
| 0 | 0.014 2 | 0.003 76 | 0.053 0 | 0.092 9 | 0.659 | 0.013 4 |
| 1 | 0.011 8 | 0.003 87 | 0.037 1 | 0.121 | 0.448 | 0.022 2 |
| 2 | 0.009 91 | 0.003 85 | 0.026 7 | 0.120 | 0.312 | 0.026 8 |
| 3 | 0.008 33 | 0.003 73 | 0.019 6 | 0.108 | 0.223 | 0.028 1 |
| 4 | 0.007 02 | 0.003 55 | 0.014 7 | 0.092 1 | 0.163 | 0.027 5 |
| 9 | 0.003 02 | 0.002 29 | 0.004 22 | 0.034 7 | 0.042 9 | 0.015 6 |
| 19 | 0.000 563 | 0.000 577 | 0.000 575 | 0.005 10 | 0.004 36 | 0.003 12 |
| 29 | 0.000 105 | 0.000 116 | 0.000 098 5 | 0.000 875 | 0.000 895 | 0.000 585 |
| 39 | 0.000 019 0 | 0.000 021 8 | 0.000 017 9 | 0.000 159 | 0.000 162 | 0.000 109 |
| 49 | - | - | - | 0.000 029 0 | 0.000 029 5 | 0.000 020 0 |

APPENDIX F

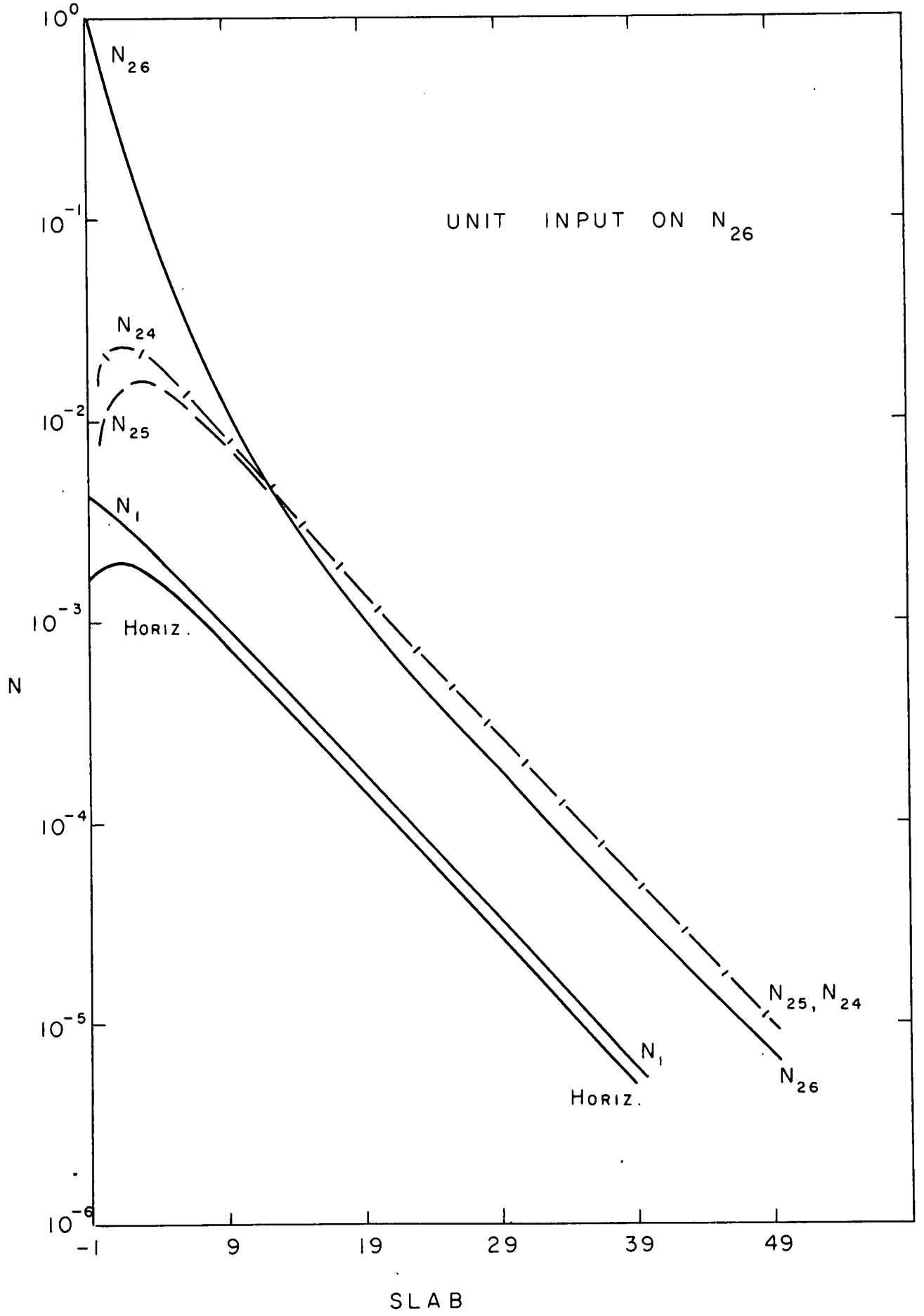
UNIT INPUT ON $N_{26}$
$N_{26}$
$N_{24}$
$N_{25}$
$N_1$
HORIZ.
$N_{25}, N_{24}$
$N_1$
HORIZ.
$N_{26}$
N
SLAB
$10^0$
$10^{-1}$
$10^{-2}$
$10^{-3}$
$10^{-4}$
$10^{-5}$
$10^{-6}$
-1
9
19
29
39
49

APPENDIX F

$N_{26}$

| Slab | $N_1$ | $\bar{N}_{10-17}$ | $N_{24}$ | $N_{25}$ | $N_{26}$ |
|---|---|---|---|---|---|
| -1 | 0.004 28 | 0.001 56 | 0 | 0 | 1 |
| 0 | 0.003 80 | 0.001 91 | 0.017 0 | 0.008 32 | 0.600 |
| 1 | 0.003 33 | 0.002 00 | 0.022 5 | 0.013 1 | 0.362 |
| 2 | 0.002 90 | 0.001 93 | 0.022 8 | 0.015 2 | 0.220 |
| 3 | 0.002 50 | 0.001 79 | 0.021 1 | 0.015 5 | 0.135 |
| 4 | 0.002 14 | 0.001 61 | 0.018 6 | 0.014 8 | 0.084 0 |
| 9 | 0.000 954 | 0.000 780 | 0.008 17 | 0.007 81 | 0.010 7 |
| 19 | 0.000 179 | 0.000 149 | 0.001 47 | 0.001 48 | 0.001 03 |
| 29 | 0.000 032 2 | 0.000 027 7 | 0.000 270 | 0.000 274 | 0.000 186 |
| 39 | 0.000 006 02 | 0.000 005 13 | 0.000 050 0 | 0.000 050 9 | 0.000 035 4 |
| 49 | - | - | 0.000 009 19 | 0.000 009 35 | 0.000 003 63 |

APPENDIX F

PHASE 2

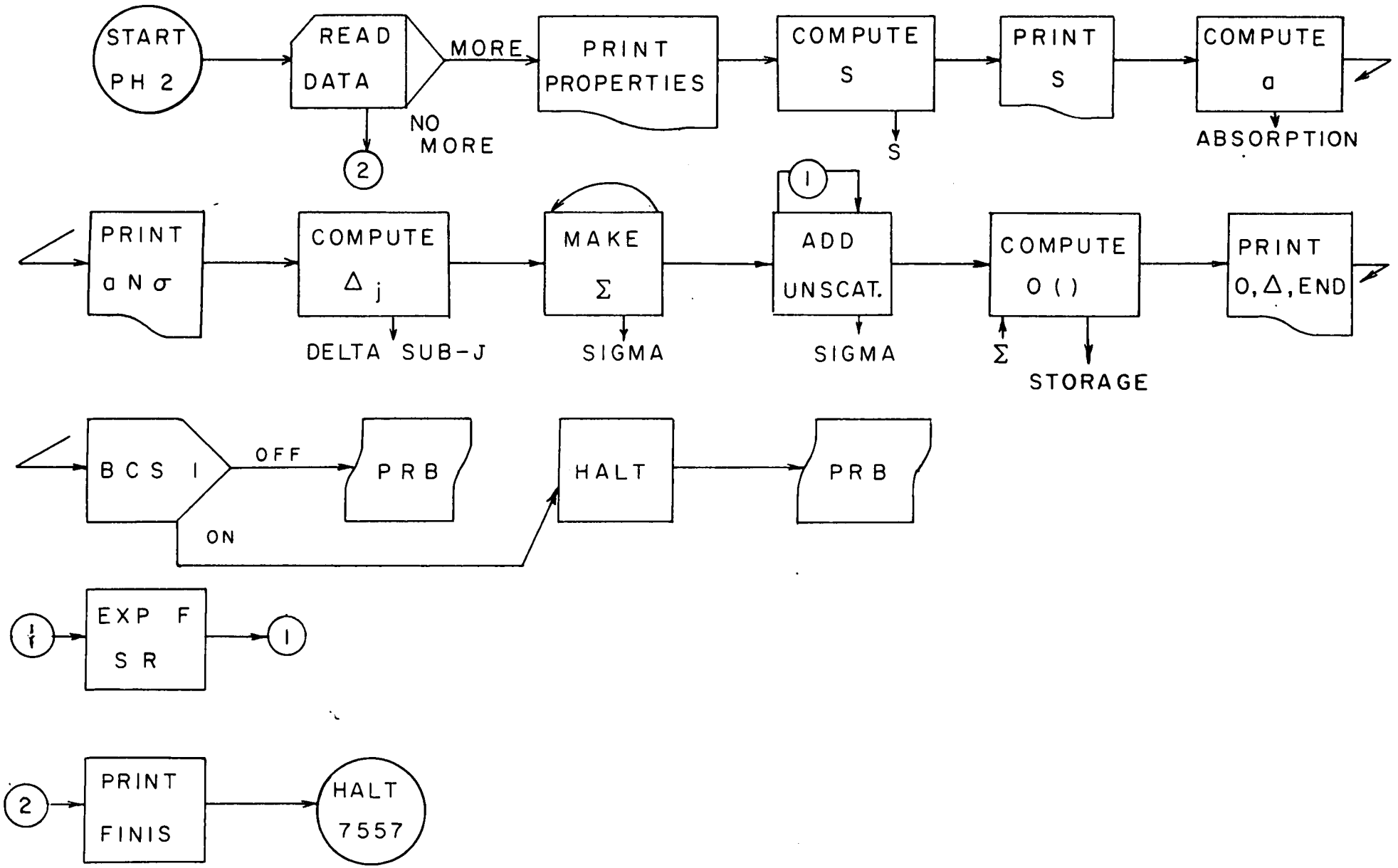
START PH 2
READ DATA
MORE
NO MORE
2
PRINT PROPERTIES
COMPUTE S
S
PRINT S
COMPUTE a
ABSORPTION
PRINT a N σ
COMPUTE Δ j
DELTA SUB-J
MAKE Σ
SIGMA
1
ADD UNSCAT.
SIGMA
COMPUTE O ( )
Σ
STORAGE
PRINT O, Δ, END
BCS 1
OFF
ON
PRB
HALT
PRB
EXP F S R
1
2
PRINT FINIS
HALT 7557

PHASE 3

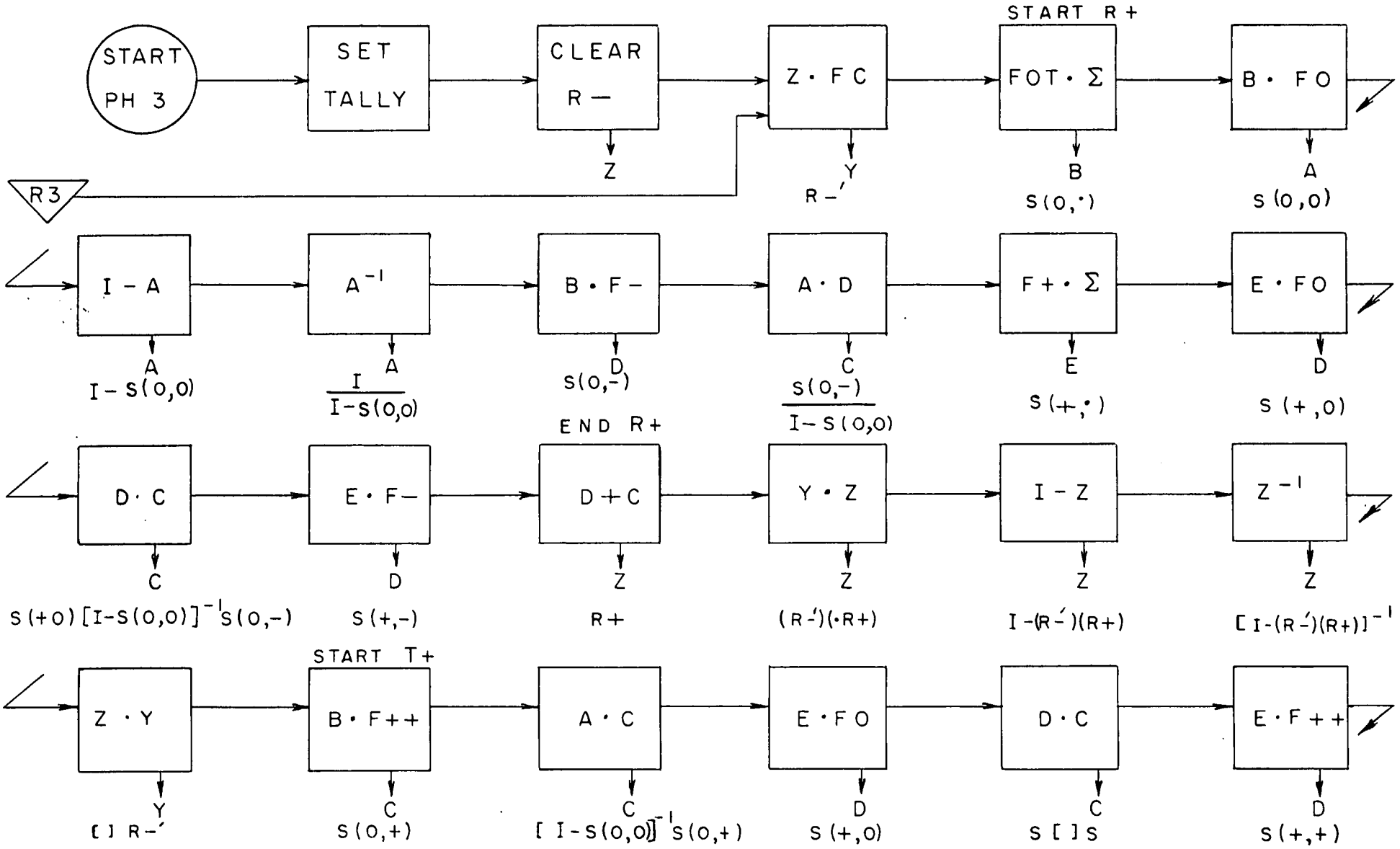


APPENDIX G

PHASE 3

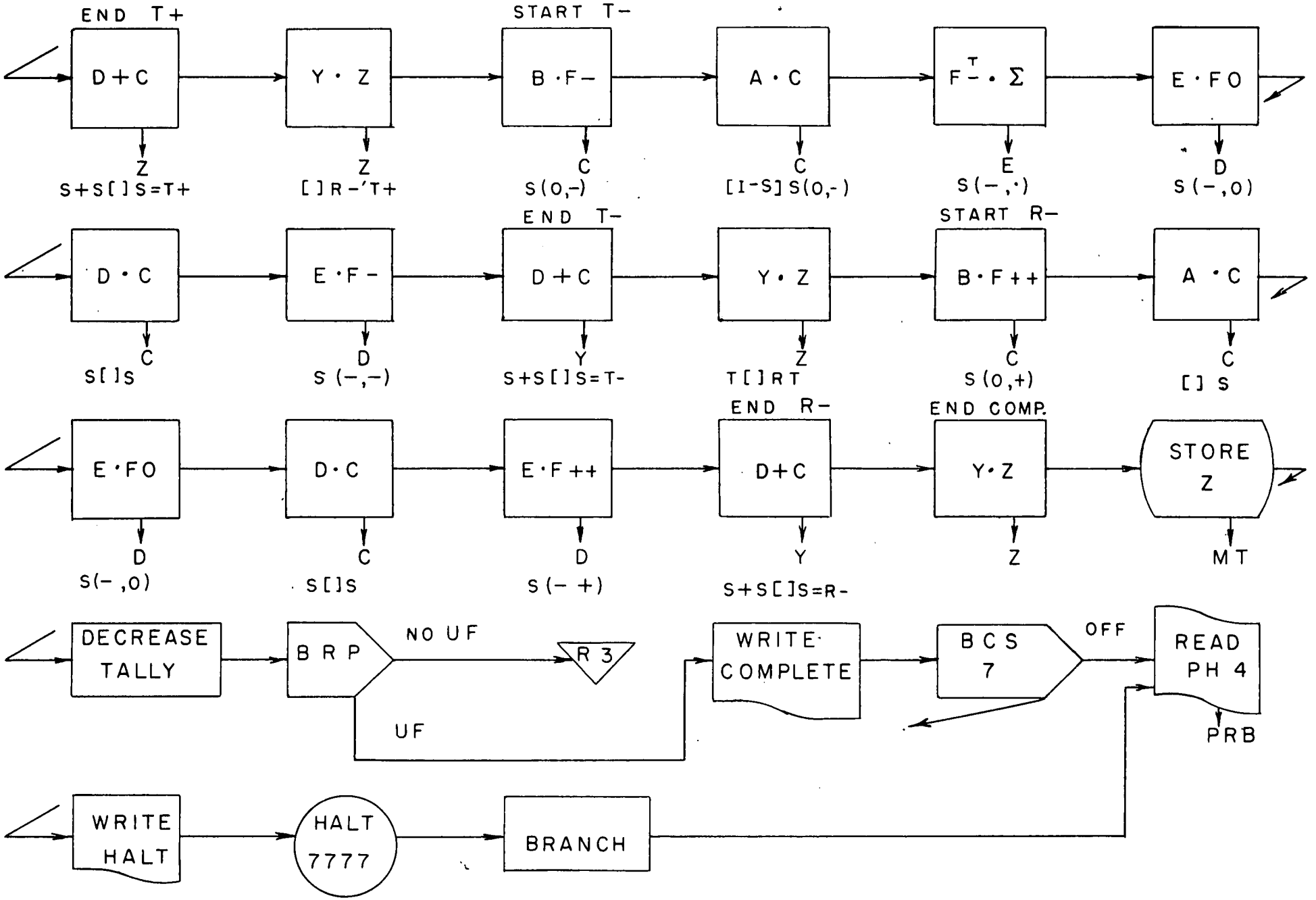
END T+
D+C
Z
S+S[]S=T+
Y · Z
Z
[]R-'T+
START T-
B · F-
C
S(0,-)
A · C
C
[I-S]S(0,-)
F T- · Σ
E
S(-,·)
E · FO
D
S(-,0)
D · C
C
S[]S
E · F-
D
S(-,-)
END T-
D+C
Y
S+S[]S=T-
Y · Z
Z
T[]RT
START R-
B · F++
C
S(0,+)
A · C
C
[] S
E · FO
D
S(-,0)
D · C
C
S[]S
E · F++
D
S(-+)
END R-
D+C
Y
S+S[]S=R-
END COMP.
Y · Z
Z
STORE Z
MT
DECREASE TALLY
B R P
NO UF
R 3
UF
WRITE COMPLETE
BCS 7
OFF
READ PH 4
PRB
WRITE HALT
HALT 7777
BRANCH

## PHASE 4

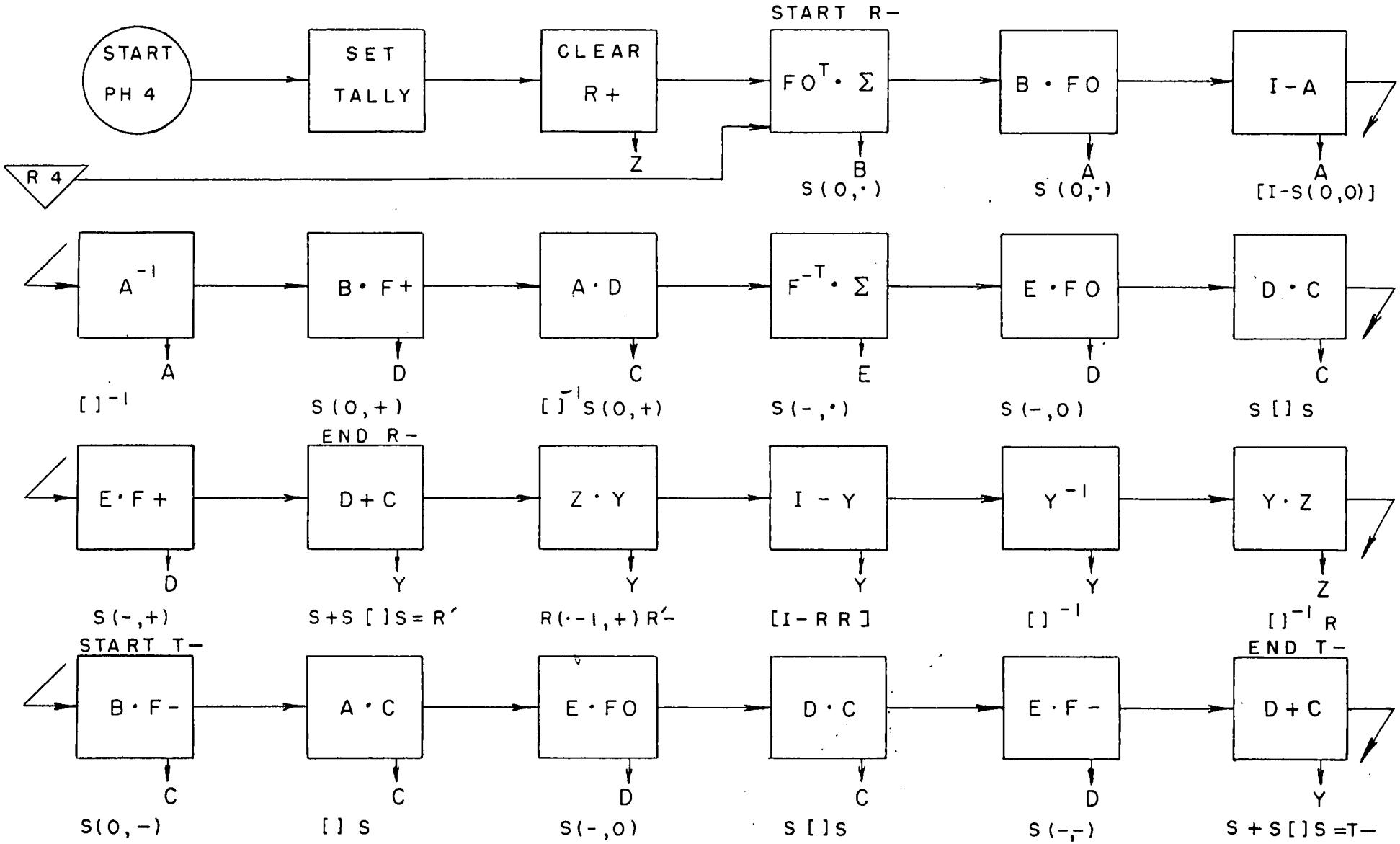


APPENDIX G

PHASE 4

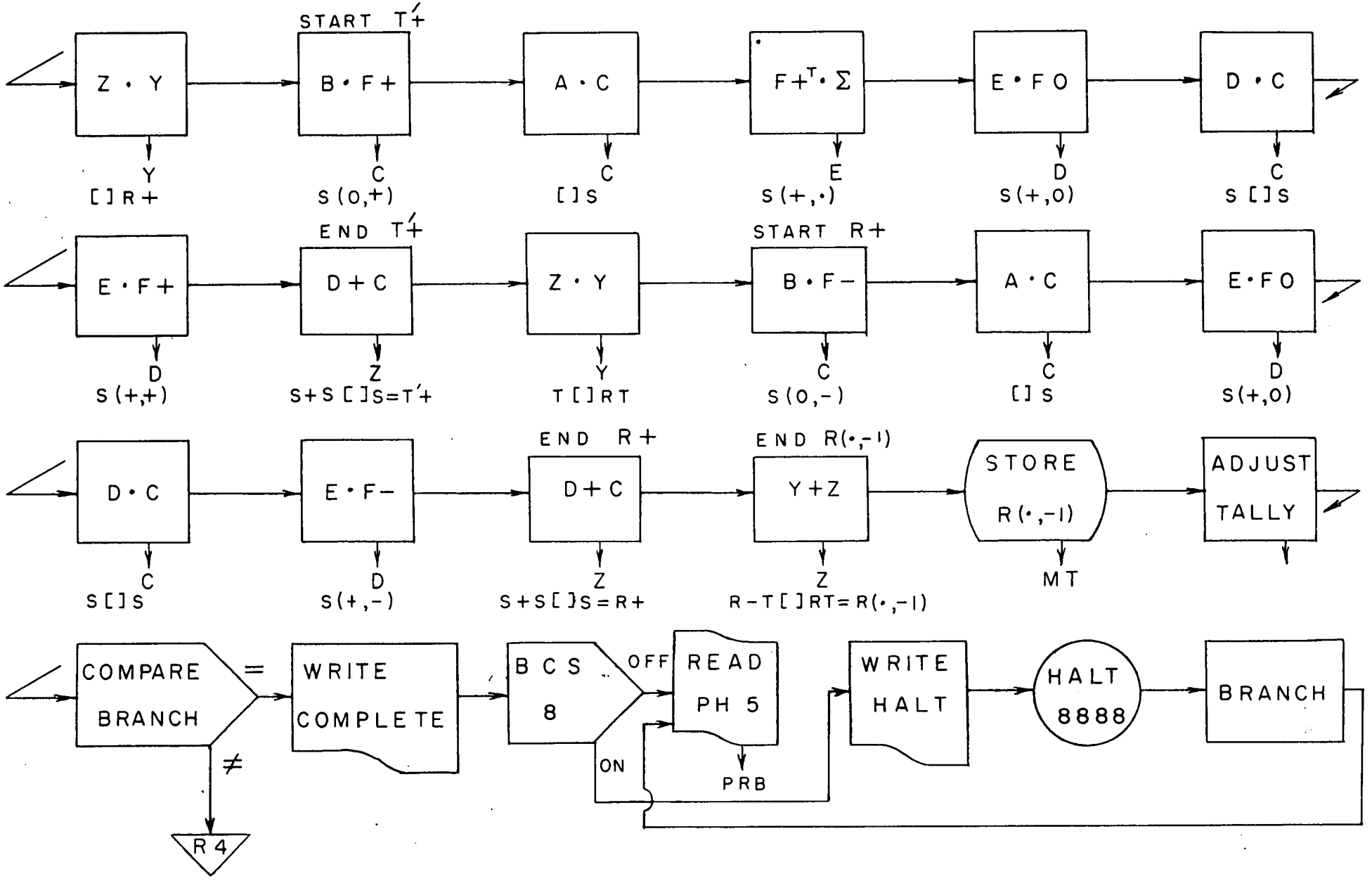
Z · Y
Y
[]R+
START T′+
B · F+
C
S(0,+)
A · C
C
[]S
F+T · Σ
E
S(+,·)
E · F O
D
S(+,0)
D · C
C
S []S
E · F+
D
S(+,+)
END T′+
D+C
Z
S+S []S=T′+
Z · Y
Y
T []RT
START R+
B · F−
C
S(0,−)
A · C
C
[] S
E·FO
D
S(+,0)
D · C
C
S[]S
E · F−
D
S(+,−)
END R+
D+C
Z
S+S[]S=R+
END R(·,−1)
Y+Z
Z
R−T[]RT=R(·,−1)
STORE
R(·,−1)
MT
ADJUST
TALLY
COMPARE
BRANCH
=
≠
R 4
WRITE
COMPLETE
B C S
8
OFF
ON
READ
PH 5
PRB
WRITE
HALT
HALT
8888
BRANCH

## PHASE 5

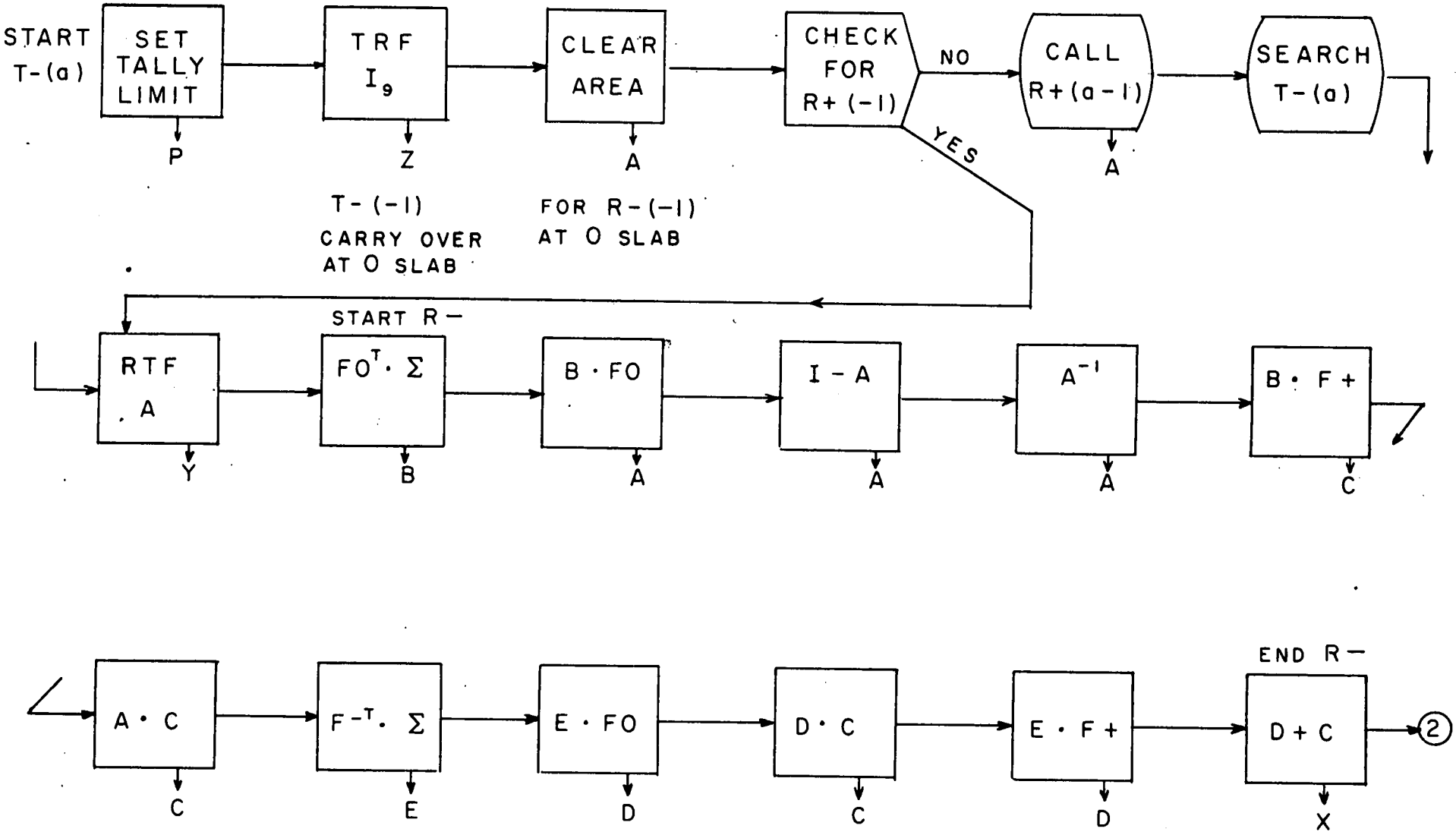


APPENDIX G



(1)

PHASE 5

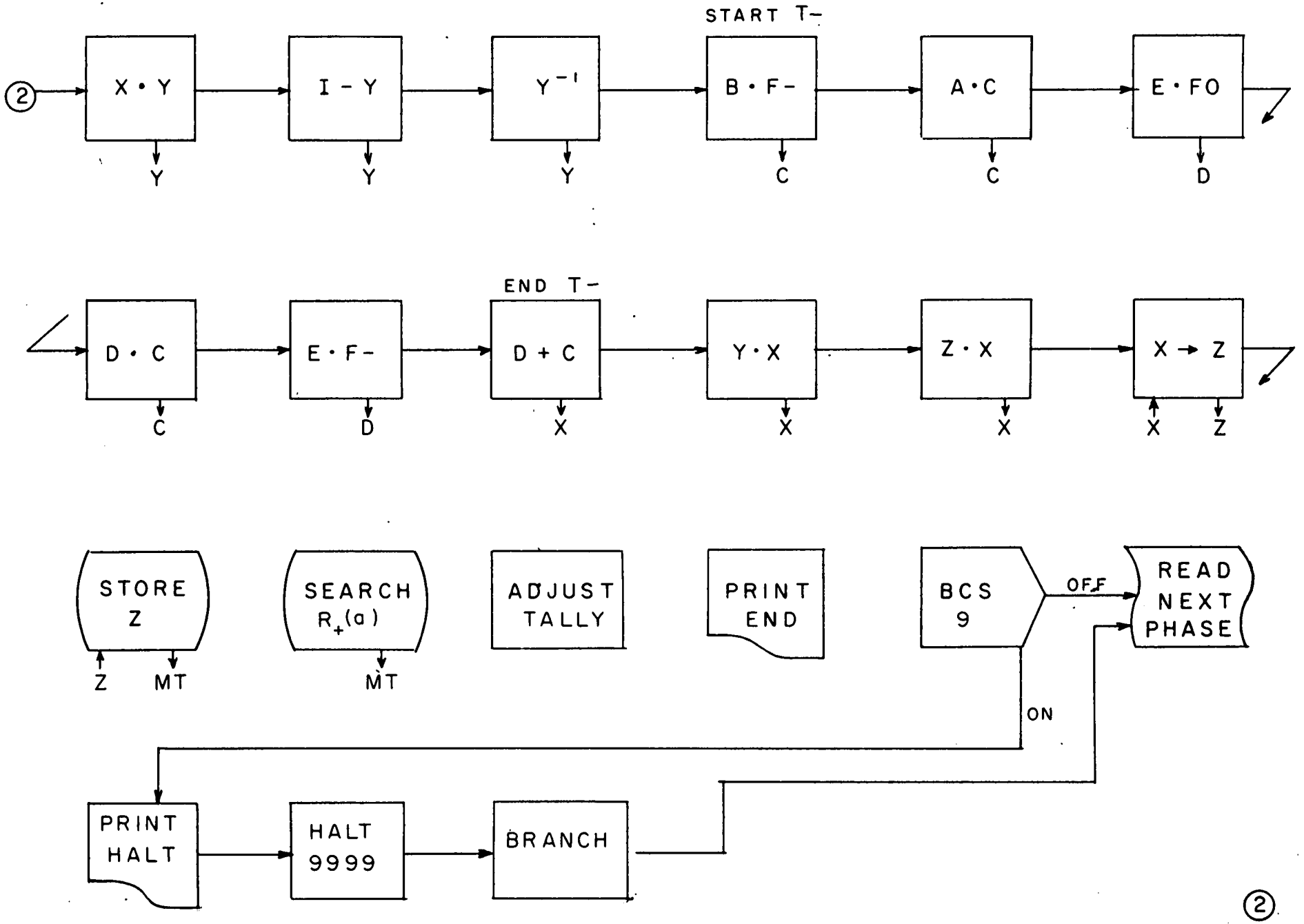
START T-
2
X • Y
I - Y
Y⁻¹
B • F-
A • C
E • FO
Y
Y
Y
C
C
D
END T-
D • C
E • F-
D + C
Y • X
Z • X
X → Z
C
D
X
X
X
X
Z
STORE Z
Z
MT
SEARCH R+(a)
MT
ADJUST TALLY
PRINT END
BCS 9
OFF
READ NEXT PHASE
ON
PRINT HALT
HALT 9999
BRANCH
2

PHASE 6

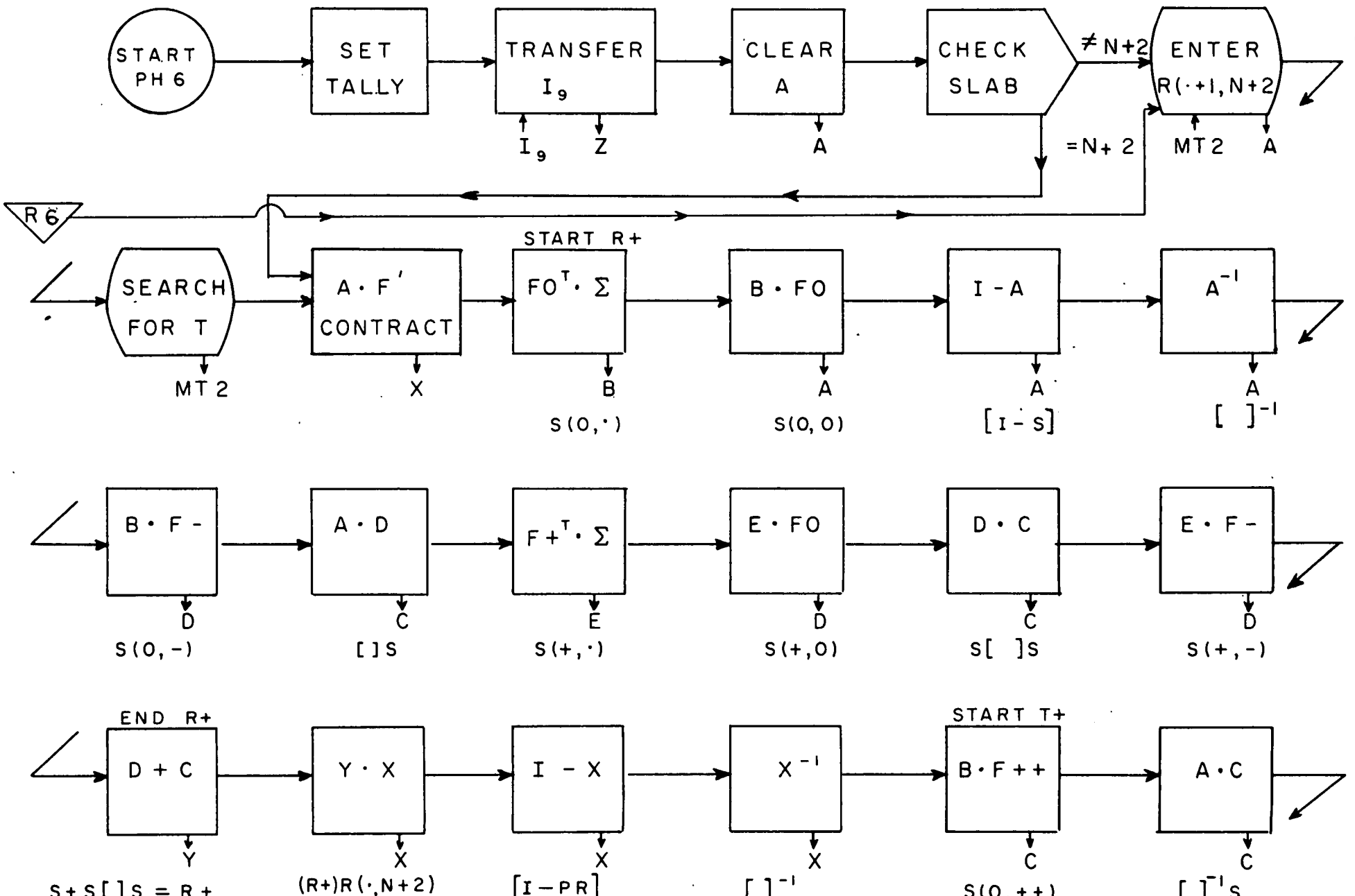
START PH 6
SET TALLY
TRANSFER $I_9$
$I_9$ Z
CLEAR A
A
CHECK SLAB
$\neq N+2$
ENTER R(·+1, N+2
MT2 A
$=N+2$
R6
SEARCH FOR T
MT 2
A · F′ CONTRACT
X
START R+
$FO^T \cdot \Sigma$
B
S(0,·)
B · FO
A
S(0, 0)
I - A
A
[I - S]
$A^{-1}$
A
$[\ ]^{-1}$
B · F -
D
S(0, -)
A · D
C
[ ]S
$F+^T \cdot \Sigma$
E
S(+,·)
E · FO
D
S(+,0)
D · C
C
S[ ]S
E · F -
D
S(+, -)
END R+
D + C
Y
S+S[ ]S = R+
Y · X
X
(R+)R(·,N+2)
I - X
X
[I - PR]
$X^{-1}$
X
$[\ ]^{-1}$
START T+
B · F++
C
S(0,++)
A · C
C
$[\ ]^{-1}$S

PHASE 6

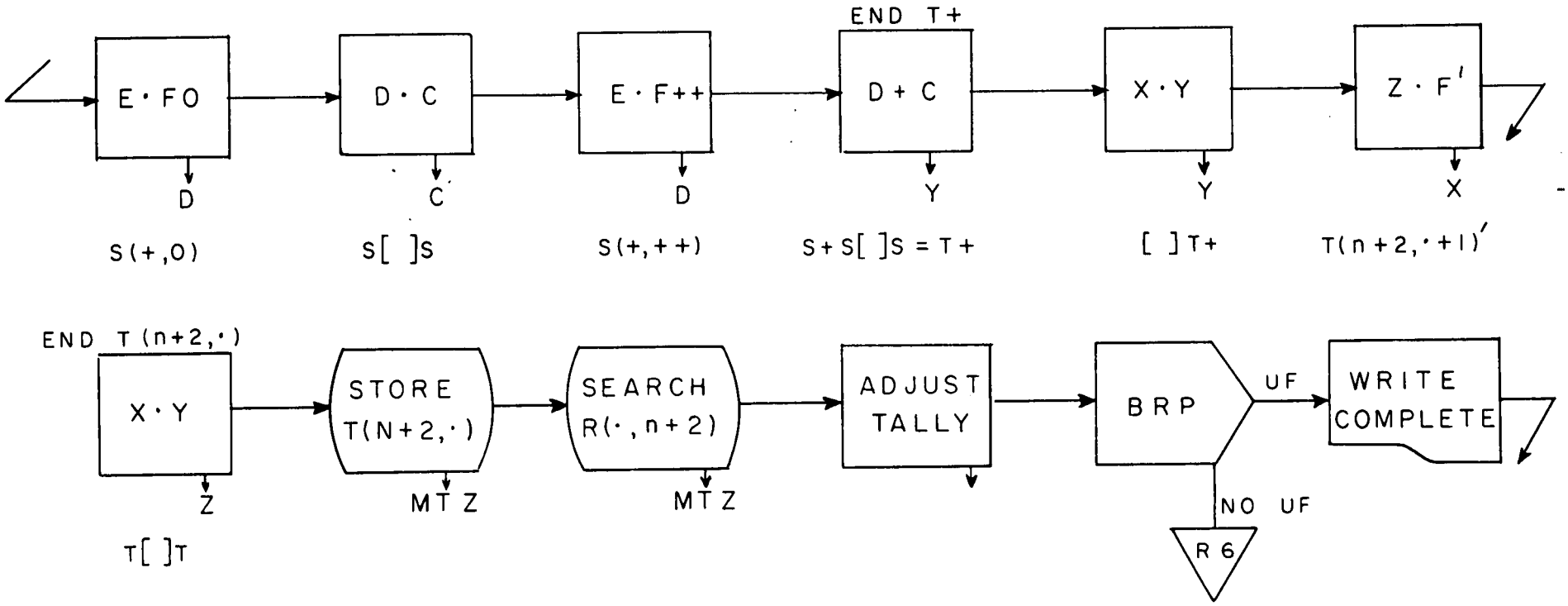
E · FO
D
S(+,0)
D · C
C
S[ ]S
E · F++
D
S(+,++)
END T+
D + C
Y
S+S[ ]S = T+
X · Y
Y
[ ]T+
Z · F'
X
T(n+2,·+1)'
END T(n+2,·)
X · Y
Z
T[ ]T
STORE T(N+2,·)
MT Z
SEARCH R(·,n+2)
MT Z
ADJUST TALLY
BRP
UF
NO UF
R 6
WRITE COMPLETE
BCS 0
OFF
READ PH 7
ON
PRB
WRITE HALT
HALT 0000
BRANCH

PHASE 7

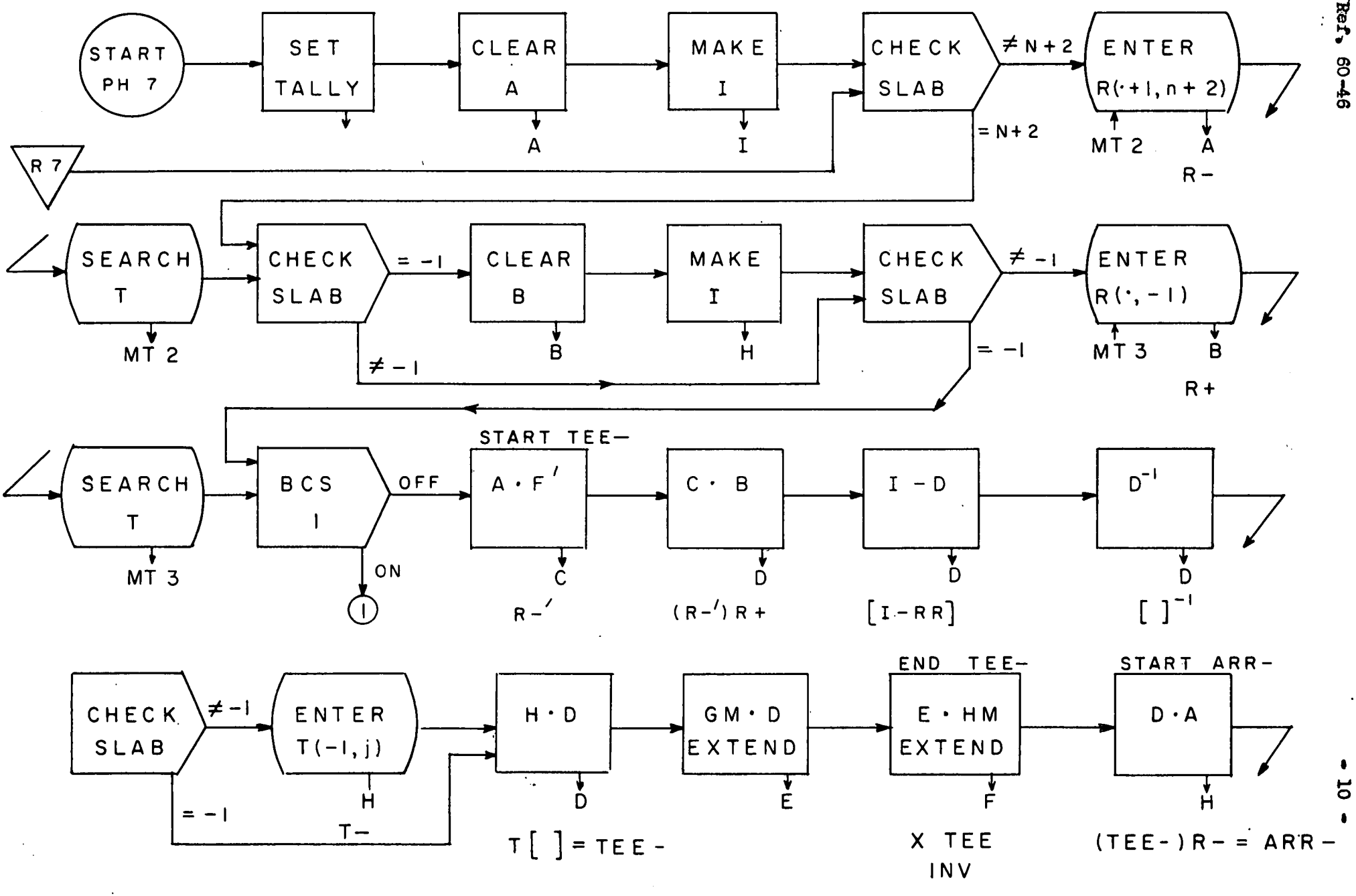
START PH 7
SET TALLY
CLEAR A
A
MAKE I
I
CHECK SLAB
≠ N+2
ENTER R(·+1, n+2)
MT 2
A
R-
= N+2
R 7
SEARCH T
MT 2
CHECK SLAB
= -1
CLEAR B
B
MAKE I
H
CHECK SLAB
≠ -1
ENTER R(·, -1)
MT 3
B
R+
≠ -1
= -1
SEARCH T
MT 3
BCS 1
OFF
ON
1
START TEE-
A · F′
C
R-′
C · B
D
(R-′)R+
I - D
D
[I-RR]
D⁻¹
D
[ ]⁻¹
CHECK SLAB
≠ -1
= -1
T-
ENTER T(-1, j)
H
H · D
D
T[ ] = TEE-
GM · D EXTEND
E
END TEE-
E · HM EXTEND
F
X TEE
INV
START ARR-
D · A
H
(TEE-)R- = ARR-

PHASE 7

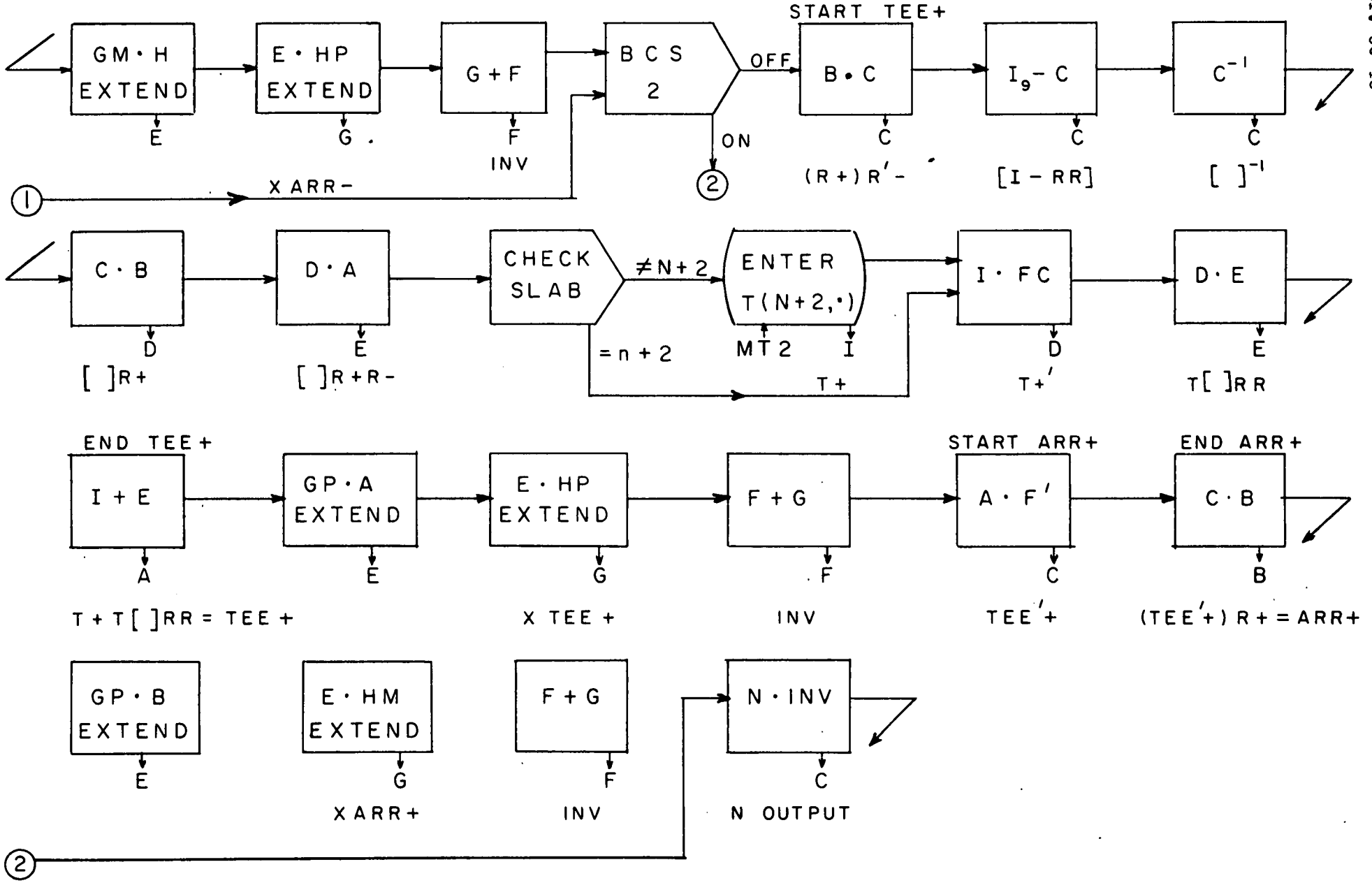
GM · H EXTEND
E
E · HP EXTEND
G
G + F
F
INV
B C S 2
OFF
ON
START TEE+
B • C
C
(R+) R'-
I9 - C
C
[I - RR]
C-1
C
[ ]-1
X ARR-
1
2
C · B
D
[ ]R+
D · A
E
[ ]R+R-
CHECK SLAB
≠N+2
=n+2
ENTER T(N+2,•)
MT2
I
T+
I · FC
D
T+'
D · E
E
T[ ]RR
END TEE+
I + E
A
T + T[ ]RR = TEE+
GP · A EXTEND
E
E · HP EXTEND
G
X TEE+
F + G
F
INV
START ARR+
A · F'
C
TEE'+
END ARR+
C · B
B
(TEE'+) R+ = ARR+
GP · B EXTEND
E
E · HM EXTEND
G
XARR+
F + G
F
INV
N · INV
C
N OUTPUT
2

PHASE 7

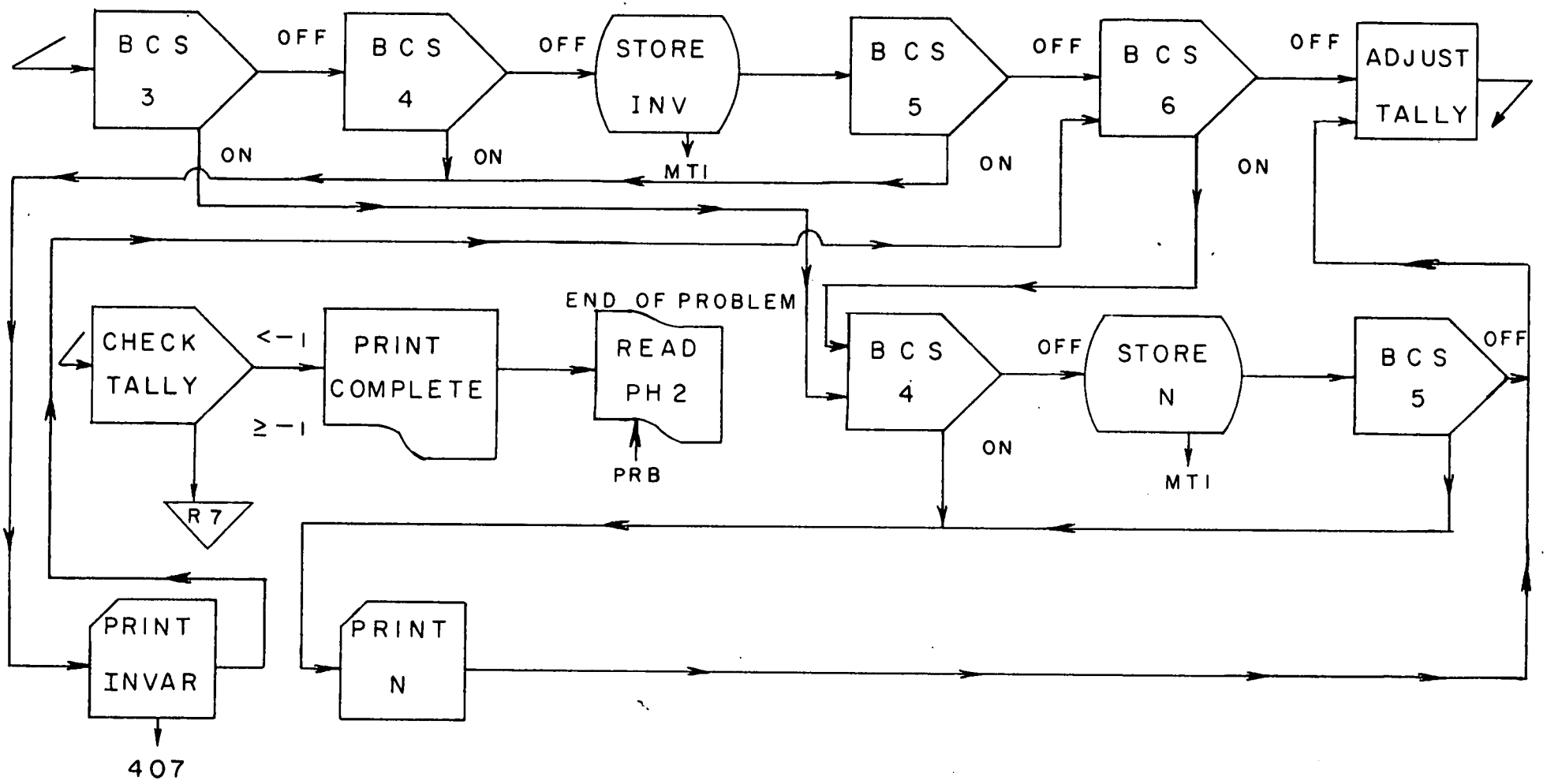
BCS 3
OFF
BCS 4
OFF
STORE INV
OFF
BCS 5
OFF
BCS 6
OFF
ADJUST TALLY
ON
ON
MTI
ON
ON
END OF PROBLEM
CHECK TALLY
<-1
≥-1
PRINT COMPLETE
READ PH 2
PRB
BCS 4
OFF
STORE N
BCS 5
OFF
ON
MTI
R 7
PRINT INVAR
PRINT N
407

## $\theta$ MATRIX

| Angle Number | Angle |
|---|---|
| 0 | 0.000 |
| 1 | 35.264 |
| 2 | 45.000 |
| 3 | 54.736 |
| 4 | 60.000 |
| 5 | 70.529 |
| 6 | 90.000 |
| 7 | 109.471 |
| 8 | 120.000 |
| 9 | 125.264 |
| 10 | 135.000 |
| 11 | 144.736 |
| 12 | 180.000 |

SCATTERING ANGLE NUMBER

| i \ k | 1 | 2 | 3 | 4 | 5 | 6 | 7 | 8 | 9 | 10 | 11 | 12 | 13 |
|---|---|---|---|---|---|---|---|---|---|---|---|---|---|
| 1 | 0 | 2 | 3 | 2 | 3 | 2 | 3 | 2 | 3 | 6 | 6 | 6 | 6 |
| 2 | 2 | 0 | 1 | 4 | 6 | 6 | 6 | 4 | 1 | 2 | 4 | 6 | 8 |
| 3 | 3 | 1 | 0 | 1 | 5 | 6 | 7 | 6 | 5 | 3 | 1 | 3 | 6 |
| 4 | 2 | 4 | 1 | 0 | 1 | 4 | 6 | 6 | 6 | 6 | 4 | 2 | 4 |
| 5 | 3 | 6 | 5 | 1 | 0 | 1 | 5 | 6 | 7 | 9 | 6 | 3 | 1 |
| 6 | 2 | 6 | 6 | 4 | 1 | 0 | 1 | 4 | 6 | 10 | 8 | 6 | 4 |
| 7 | 3 | 6 | 7 | 6 | 5 | 1 | 0 | 1 | 5 | 9 | 11 | 9 | 6 |
| 8 | 2 | 4 | 6 | 6 | 6 | 4 | 1 | 0 | 1 | 6 | 8 | 10 | 8 |
| 9 | 3 | 1 | 5 | 6 | 7 | 6 | 5 | 1 | 0 | 3 | 6 | 9 | 11 |
| 10 | 6 | 2 | 3 | 6 | 9 | 10 | 9 | 6 | 3 | 0 | 2 | 6 | 10 |
| 11 | 6 | 4 | 1 | 4 | 6 | 8 | 11 | 8 | 6 | 2 | 0 | 2 | 6 |
| 12 | 6 | 6 | 3 | 2 | 3 | 6 | 9 | 10 | 9 | 6 | 2 | 0 | 2 |
| 13 | 6 | 8 | 6 | 4 | 1 | 4 | 6 | 8 | 11 | 10 | 6 | 2 | 0 |
| 14 | 6 | 10 | 9 | 6 | 3 | 2 | 3 | 6 | 9 | 12 | 10 | 6 | 2 |
| 15 | 6 | 8 | 11 | 8 | 6 | 4 | 1 | 4 | 6 | 10 | 12 | 10 | 6 |
| 16 | 6 | 6 | 9 | 10 | 9 | 6 | 3 | 2 | 3 | 6 | 10 | 12 | 10 |
| 17 | 6 | 4 | 6 | 8 | 11 | 8 | 6 | 4 | 1 | 2 | 6 | 10 | 12 |
| 18 | 10 | 6 | 6 | 8 | 11 | 12 | 11 | 8 | 6 | 2 | 4 | 6 | 8 |
| 19 | 9 | 6 | 5 | 6 | 7 | 11 | 12 | 11 | 7 | 3 | 1 | 3 | 6 |
| 20 | 10 | 8 | 6 | 6 | 6 | 8 | 11 | 12 | 11 | 6 | 4 | 2 | 4 |
| 21 | 9 | 11 | 7 | 6 | 5 | 6 | 7 | 11 | 12 | 9 | 6 | 3 | 1 |
| 22 | 10 | 12 | 11 | 8 | 6 | 6 | 6 | 8 | 11 | 10 | 8 | 6 | 4 |
| 23 | 9 | 11 | 12 | 11 | 7 | 6 | 5 | 6 | 7 | 9 | 11 | 9 | 6 |
| 24 | 10 | 8 | 11 | 12 | 11 | 8 | 6 | 6 | 6 | 6 | 8 | 10 | 8 |
| 25 | 9 | 6 | 7 | 11 | 12 | 11 | 7 | 6 | 5 | 3 | 6 | 9 | 11 |
| 26 | 12 | 10 | 9 | 10 | 9 | 10 | 9 | 10 | 9 | 6 | 6 | 6 | 6 |

SCATTERING ANGLE NUMBER (Cont)

| i \ k | 14 | 15 | 16 | 17 | 18 | 19 | 20 | 21 | 22 | 23 | 24 | 25 | 26 |
|---|---|---|---|---|---|---|---|---|---|---|---|---|---|
| 1 | 6 | 6 | 6 | 6 | 10 | 9 | 10 | 9 | 10 | 9 | 10 | 9 | 12 |
| 2 | 10 | 8 | 6 | 4 | 6 | 6 | 8 | 11 | 12 | 11 | 8 | 6 | 10 |
| 3 | 9 | 11 | 9 | 6 | 6 | 5 | 6 | 7 | 11 | 12 | 11 | 7 | 9 |
| 4 | 6 | 8 | 10 | 8 | 8 | 6 | 6 | 6 | 8 | 11 | 12 | 11 | 10 |
| 5 | 3 | 6 | 9 | 11 | 11 | 7 | 6 | 5 | 6 | 7 | 11 | 12 | 9 |
| 6 | 2 | 4 | 6 | 8 | 12 | 11 | 8 | 6 | 6 | 6 | 8 | 11 | 10 |
| 7 | 3 | 1 | 3 | 6 | 11 | 12 | 11 | 7 | 6 | 5 | 6 | 7 | 9 |
| 8 | 6 | 4 | 2 | 4 | 8 | 11 | 12 | 11 | 8 | 6 | 6 | 6 | 10 |
| 9 | 9 | 6 | 3 | 1 | 6 | 7 | 11 | 12 | 11 | 7 | 6 | 5 | 9 |
| 10 | 12 | 10 | 6 | 2 | 2 | 3 | 6 | 9 | 10 | 9 | 6 | 3 | 6 |
| 11 | 10 | 12 | 10 | 6 | 4 | 1 | 4 | 6 | 8 | 11 | 8 | 6 | 6 |
| 12 | 6 | 10 | 12 | 10 | 6 | 3 | 2 | 3 | 6 | 9 | 10 | 9 | 6 |
| 13 | 2 | 6 | 10 | 12 | 8 | 6 | 4 | 1 | 4 | 6 | 8 | 11 | 6 |
| 14 | 0 | 2 | 6 | 10 | 10 | 9 | 6 | 3 | 2 | 3 | 6 | 9 | 6 |
| 15 | 2 | 0 | 2 | 6 | 8 | 11 | 8 | 6 | 4 | 1 | 4 | 6 | 6 |
| 16 | 6 | 2 | 0 | 2 | 6 | 9 | 10 | 9 | 6 | 3 | 2 | 3 | 6 |
| 17 | 10 | 6 | 2 | 0 | 4 | 6 | 8 | 11 | 8 | 6 | 4 | 1 | 6 |
| 18 | 10 | 8 | 6 | 4 | 0 | 1 | 4 | 6 | 6 | 6 | 4 | 1 | 2 |
| 19 | 9 | 11 | 9 | 6 | 1 | 0 | 1 | 5 | 6 | 7 | 6 | 5 | 3 |
| 20 | 6 | 8 | 10 | 8 | 4 | 1 | 0 | 1 | 4 | 6 | 6 | 6 | 2 |
| 21 | 3 | 6 | 9 | 11 | 6 | 5 | 1 | 0 | 1 | 5 | 6 | 7 | 3 |
| 22 | 2 | 4 | 6 | 8 | 6 | 6 | 4 | 1 | 0 | 1 | 4 | 6 | 2 |
| 23 | 3 | 1 | 3 | 6 | 6 | 7 | 6 | 5 | 1 | 0 | 1 | 5 | 3 |
| 24 | 6 | 4 | 2 | 4 | 4 | 6 | 6 | 6 | 4 | 1 | 0 | 1 | 2 |
| 25 | 9 | 6 | 3 | 1 | 1 | 5 | 6 | 7 | 6 | 5 | 1 | 0 | 3 |
| 26 | 6 | 6 | 6 | 6 | 2 | 3 | 2 | 3 | 2 | 3 | 2 | 3 | 0 |

APPENDIX H